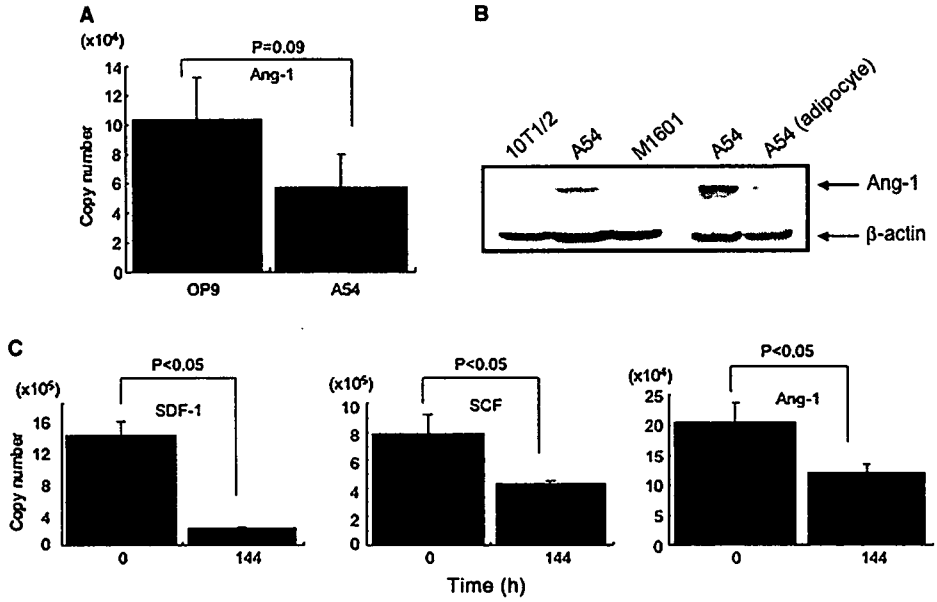

Figure 4. Ang-1 expression and down-regulation of SCF, SDF-1 and Ang-1 in A54 cells after adipocyte differentiation. (A) The level of Ang-1 mRNA in A54 cells was similar to that in OP9 cells, a well-characterized stromal cell line that supports the survival of hematopoietic stem cells. (B) Western blot analysis of Ang-1 protein expression among 10T1/2, A54, M1601 and A54 cells differentiated into adipocytes. (C) The changes in levels of SCF, SDF-1 and Ang-1 mRNA in A54 cells before and after adipocyte differentiation were monitored by real-time PCR. The copy number was used to compare the level of expression. The mean ± SD from three independent reactions using the same cDNA is

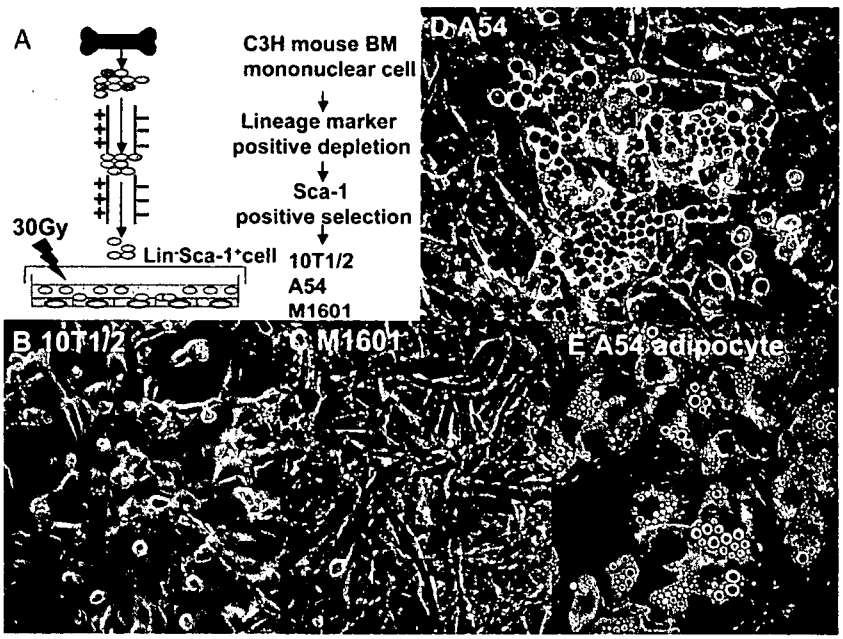

Figure 5. Formation of cobblestone appearance on 10T1/2, A54 and M1601 cells. (A) Experimental procedure. (B–E) 10T1/2, A54 and M1601 were co-cultured with a mouse hematopoietic stem cell fraction for 6 days. The formation of cobblestone appearance was evaluated by phase-contrast microscopy.

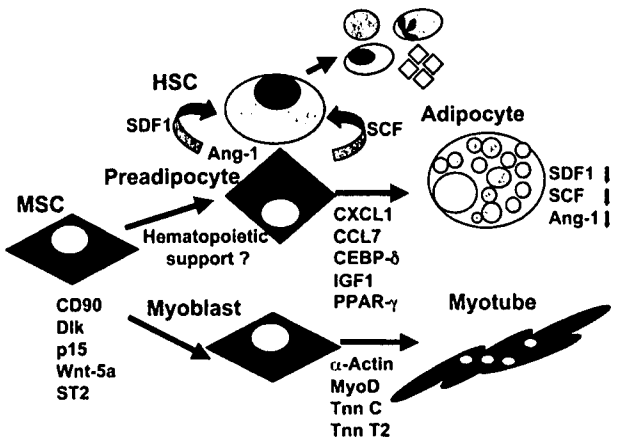

Figure 6. Proposed model for the hierarchy of the BM stromal system. Schematic relationship among MSC, pre-adipocytes and myoblasts and the up-regulated genes in each cell. The expression of CD90, Dlk, Wnt-5a and ST2 was up-regulated in 10T1/2 cells. The up-regulated genes in A54 (SCF, SDF-1, and Ang-1) were suppressed after adipocyte differentiation. The expression of α-actin, MyoD, troponin C and troponin T2 was up-regulated in M1601 cells.

PCR. As shown in Figure 4C, the expression of these genes decreased after the adipocyte differentiation.

Up-regulation of troponin T2 gene in M1601 cells

We confirmed that the expression of *cardiac troponin T2* was up-regulated in M1601 cells (Figure 2C). Figure 2D demonstrates that the level of β-actin expression in each line was almost the same.

Discussion

In the current studies, we used 10T1/2 and two 10T1/2-derived cell lines as models of MSC and progenitor cells. The genes regulating MSC differentiation remain obscure. Because primary MSC may contain heterogeneous progenitors and because the extent of differentiation may vary, it is difficult to use them for high-throughput analysis of gene expression. Therefore, we chose these three cell lines to avoid problems related to the heterogeneity of MSC; all three cell lines had the same genetic background because the A54 and M1601 cells were both derived from 10T1/2 cells.

Up-regulation of *Dlk* in 10T1/2 cells was confirmed by micro-array and RT real-time PCR. Although *Dlk* has been reported to inhibit adipocyte and osteoblast differentiation [16], overexpression of *Dlk* did not affect adipocyte differentiation of A54 cells. This is not surprising because other factor(s) may also be required for the inhibition of differentiation.

Wnt-5a is a member of the Wnt family, which plays an essential role in regulating proliferation and differentiation [19]. Our GeneChip analysis demonstrated that *Wnt-5a* was expressed in parental 10T1/2 cells and that the gene expression of its receptor, Frizzled, was up-regulated in the downstream progenitor cell line, A54. MSC may self-regulate their differentiation or proliferation in the BM through the Wnt-5a signaling system. The genes up-regulated in the parental 10T1/2 cells, namely, *Dlk*, *Wnt-5a*, *ST2*, *Crbpl*, *p15* and *CD90*, may be worth investigating further to identify molecules important for maintaining stemness.

SCF and *SDF-1* were exclusively up-regulated in A54 pre-adipocyte cells. This agreed with the ability of these cells to support hematopoietic cell growth. Adipocyte differentiation down-regulated the expression of these genes and reduced the ability of the A54 cells to support hematopoietic cell growth. These results indicate that pre-adipocytes may be one of the committed progenitors that participate in hematopoietic support and that the loss of this ability after terminal adipocyte differentiation may be involved in a fatty change of BM in aging or aplastic anemia. Ang-1 has been reported to be essential for the self-renewal of hematopoietic stem cells and to be expressed on osteoblasts in the BM niche [14]. Our results suggested that both pre-adipocytes and osteoblasts in the BM are Ang-1-producing cells. Pre-adipocytes appear to be related to osteoblasts because they express the mRNA for osteoblast-specific genes such as *osteocalcin* [26]. This suggests that there is a common molecular pathway in osteoblast and pre-adipocyte differentiation. Also, TAZ has been reported to be a key regulator of MSC differentiation. This protein enhances the differentiation of MSC into osteoblasts by activating Runx2 and suppresses the differentiation into adipocytes by inhibiting PPAR-γ [10].

We found that M1601 cells express *cardiac muscle-specific* gene, suggesting a possible plasticity of MSC to differentiate into cardiac muscle cells. In this study, we did not analyze the up-regulated genes in M1601 further. Human MSC differentiate into cardiac muscle cells *in vitro* upon treatment with 5-azacytidine and co-culture with primary mouse cardiac muscle cells [27]. A recent study demonstrated that allogenic MSC ameliorated cardiac function in pig myocardial infarction and rat dilated cardiomyopathy

models, suggesting that MSC have the potential to treat myocardial infarction and cardiomyopathy [28,29].

In Figure 6, we show our hypothesis of lineage- and stage-specific gene expression patterns in MSC and committed progenitors. The characterization of the transcriptional profiles should enhance the understanding of the molecular mechanisms underlying the differentiation of MSC into progenitors. Furthermore, we hypothesize that each progenitor has a unique function in BM. Our analysis has demonstrated a possible molecular mechanism of hematopoietic support by pre-adipocytes, and we found that pre-adipocyte progenitors may be better than MSC for hematopoietic engraftment in BM transplantation. Finally, because MSC contains heterogeneous progenitors and each committed progenitor has a different function in BM, the three cell lines analyzed here could be useful tools for characterizing the behavior and function of MSC.

References

1 Pittenger MF, Mackay AM, Beck SC. Multilineage potential of adult human mesenchymal stem cells. *Science* 1999;284:143–7.

2 Bensidhoum M, Chapel A, Francois S *et al.* Homing of *in vitro* expanded Stro-1$^-$ or Stro-1$^+$ human mesenchymal stem cells into the NOD/SCID mouse and their role in supporting human CD34 cell engraftment. *Blood* 2004;103:3313–9.

3 Maitra B, Szekely E, Gjini K *et al.* Human mesenchymal stem cells support unrelated donor hematopoietic stem cells and suppress T-cell activation. *Bone Marrow Transplant* 2004;33:597–604.

4 Zappia E, Casazza S, Pedemonte E *et al.* Mesenchymal stem cells ameliorate experimental autoimmune encephalomyelitis inducing T cell anergy. *Blood* 2005;106:1755–61.

5 Djouad F, Plence P, Bony C *et al.* Immunosuppressive effect of mesenchymal stem cells favors tumor growth in allogeneic animals. *Blood* 2003;102:3837–44.

6 Le Blanc K, Rasmusson I, Sundberg B *et al.* Treatment of severe acute graft-versus-host disease with third party haploidentical mesenchymal stem cells. *The Lancet* 2004;363:1439–41.

7 Lazarus HM, Koc ON, Devine SM *et al.* Cotransplantation of HLA-identical sibling culture-expanded mesenchymal stem cells and hematopoietic stem cells in hematologic malignancy patients. *Biol Blood Marrow Transplant* 2005;11:389–98.

8 Horwitz EM, Prockop DJ, Fitzpatrick LA *et al.* Transplantability and therapeutic effects of bone marrow-derived mesenchymal cells in children with osteogenesis imperfecta. *Nat Med* 1999;5:309–13.

9 Bang OY, Lee JS, Lee PH *et al.* Autologous mesenchymal stem cell transplantation in stroke patients. *Ann Neurol* 2005;57:874–82.

10 Hong JH, Hwang ES, McManus MT *et al.* TAZ, a transcriptional modulator of mesenchymal stem cell differentiation. *Science* 2005;309:1074–8.

11 Taylor SM, Jones PA. Multiple new phenotypes induced in 10T1/2 and 3T3 cells treated with 5-azacytidine. *Cell* 1979;17:771–9.

12 Nishikawa M, Ozawa K, Tojo A *et al.* Changes in hematopoiesis-supporting ability of C3H10T1/2 mouse embryo fibroblasts during differentiation. *Blood* 1993;81:1184–92.

13 Kopp HG, Avecilla ST, Hooper AT *et al.* Tie2 activation contributes to hemangiogenic regeneration after myelosuppression. *Blood* 2005;106:505–13.

14 Arai F, Hirao A, Ohmura M *et al.* Tie2/angiopoietin-1 signaling regulates hematopoietic stem cell quiescence in the bone marrow niche. *Cell* 2004;118:149–61.

15 Kume A, Xu R, Ueda Y *et al.* Long-term tracking of murine hematopoietic cells transduced with a bicistronic retrovirus containing CD24 and EGFP genes. *Gene Ther* 2000;14:1193–9.

16 Abdallah BM, Jensen CH, Gutierrez G *et al.* Regulation of human skeletal stem cells differentiation by Dlk1/Pref-1. *J Bone Miner Res* 2004;19:841–52.

17 Sakamoto K, Yamaguchi S, Ando R *et al.* The nephroblastoma overexpressed gene (NOV/ccn3) protein associates with Notch1 extracellular domain and inhibits myoblast differentiation via Notch signaling pathway. *J Biol Chem* 2002;277:29399–405.

18 Schoonjans K, Staels B, Auwerx J. The peroxisome proliferator activated receptors (PPARS) and their effects on lipid metabolism and adipocyte differentiation. *Biochim Biophys Acta* 1996;130:93–109.

19 Bennett CN, Ross SE, Longo KA *et al.* Regulation of Wnt signaling during adipogenesis. *J Biol Chem* 2002;277:30998–1004.

20 Lijnen HR, Alessi MC, Van Hoef B *et al.* On the role of plasminogen activator inhibitor-1 in adipose tissue development and insulin resistance in mice. *J Thromb Haemost* 2005;3:1174–9.

21 Kumar S, Leontovich A, Coenen MJ *et al.* Gene expression profiling of orbital adipose tissue from patients with Graves' ophthalmopathy: a potential role for secreted frizzled-related protein-1 in orbital adipogenesis. *J Clin Endocrinol Metab* 2005;90:4730–5.

22 Lassar AB, Buskin JN, Lockshon D *et al.* MyoD is a sequence-specific DNA binding protein requiring a region of myc homology to bind to the muscle creatine kinase enhancer. *Cell* 1989;58:823–31.

23 Cooper TA, Ordahl CP. A single troponin T gene regulated by different programs in cardiac and skeletal muscle development. *Science* 1984;226:979–82.

24 Maekawa TL, Takahashi TA, Fujihara M *et al.* A novel gene (drad-1) expressed in hematopoiesis-supporting stromal cell lines, ST2, PA6 and A54 preadipocytes: use of mRNA differential display. *Stem Cells* 1997;15:334–9.

25 Mazini L, Wunder E, Sovalat H *et al.* Mature accessory cells influence long-term growth of human hematopoietic progenitors on a murine stromal cell feeder layer. *Stem Cells* 1998;16:404–12.

26 Dorheim MA, Sullivan M, Dandapani V *et al*. Osteoblastic gene expression during adipogenesis in hematopoietic supporting murine bone marrow stromal cells. *J Cell Physiol* 1993;154:317–28.

27 Shim WS, Jiang S, Wong P *et al*. Ex vivo differentiation of human adult bone marrow stem cells into cardiomyocyte-like cells. *Biochem Biophys Res Commun* 2004;324:481–8.

28 Amado LC, Saliaris AP, Schuleri KH *et al*. Cardiac repair with intramyocardial injection of allogeneic mesenchymal stem cells after myocardial infarction. *Proc Natl Acad Sci USA* 2005;102:11474–9.

29 Nagaya N, Kangawa K, Itoh T *et al*. Transplantation of mesenchymal stem cells improves cardiac function in a rat model of dilated cardiomyopathy. *Circulation* 2005;112:1128–35.

30 Nakano T, Kodama H, Honjo T. *In vitro* development of primitive and definitive erythrocytes from different precursors. *Science* 1996;272:722–4.

International Journal of
HEMATOLOGY

Overexpression of Interleukin 21 Induces Expansion of Hematopoietic Progenitor Cells

Katsutoshi Ozaki,[a,e] Ai Hishiya,[a] Keiko Hatanaka,[e] Hideaki Nakajima,[b] Gang Wang,[c] Patrick Hwu,[c] Toshio Kitamura,[b] Keiya Ozawa,[e] Warren J. Leonard,[d] Tetsuya Nosaka[a]

[a]Division of Hematopoietic Factors and [b]Department of Cellular Therapy, The Institute of Medical Science, The University of Tokyo, Tokyo, Japan; [c]Department of Melanoma Medical Oncology, The University of Texas M. D. Anderson Cancer Center, Houston, Texas, USA; [d]Laboratory of Molecular Immunology, National Heart, Lung, and Blood Institute, National Institutes of Health, Bethesda, Maryland, USA; [e]Division of Hematology, Jichi Medical University, Tochigi, Japan

Received February 8, 2006; received in revised form May 30, 2006; accepted June 16, 2006

Abstract

The interleukin 21 (IL-21) receptor is expressed on T-cells, B-cells, and natural killer cells, and IL-21 is critical for regulating immunoglobulin production in vivo in cooperation with IL-4. So far, however, little is known about a role for IL-21 outside the immune system. We investigated the effect of IL-21 on hematopoiesis in vivo by using the hydrodynamics gene-delivery method. Overexpression of IL-21 increases Sca-1$^+$ cells in the periphery and spleen. It also increases the numbers of c-Kit$^+$, Sca-1$^+$, and lineage$^{-/low}$ (KSL) cells and colony-forming units–granulocyte-macrophage (CFU-GM) in the spleen, indicating the expansion of hematopoietic progenitor cells. We found that even in RAG2$^{-/-}$ mice, which lack mature T-cells and B-cells, IL-21 induced an increase in KSL cells and CFU-GM in the spleen. These results demonstrate that IL-21 can induce the expansion of hematopoietic progenitor cells in vivo, even in the absence of mature T-cells and B-cells.
Int J Hematol. 2006;84:224-230. doi: 10.1532/IJH97.06036

Key words: Interleukin 21; Hematopoietic progenitor cells; Overexpression; Expansion; CFU-GM

1. Introduction

Interleukin 21 (IL-21) is a cytokine produced by CD4$^+$ T-cells [1] that acts on T-cells, B-cells, and natural killer (NK) cells [1,2]. Like the receptor complexes for IL-2, IL-4, IL-7, IL-9, and IL-15, the receptor for IL-21 contains the common cytokine receptor γ chain (γc) [3,4]. IL-21 augments T-cell proliferation in response to T-cell receptor signaling, augments B-cell proliferation by anti-CD40, and induces the expansion, differentiation, and apoptosis of NK cells [1,5]. IL-21, together with IL-4, plays a critical role in regulating immunoglobulin production [6]. IL-21 can also promote B-cell apoptosis but nevertheless drives terminal B-cell differentiation to plasma cells [7]. IL-21 overexpression exhibits antitumor activity in vivo [8], and this effect is greater when IL-21 is combined with IL-15 [9,10]. A role for IL-21 has also been implicated in autoimmune disease [11].

The effect of IL-21 on hematopoietic cells is unknown. Previously, we established an IL-21–overexpression system in vivo [8], and we have used this system in the present study to investigate the action of IL-21 in the hematopoietic system. The hematopoietic stem cell compartment is known to express many kinds of cytokine receptors [12]. The common cytokine receptor γc is one such receptor, and this protein and the IL-21 receptor (IL-21R) comprise the functional IL-21 heterodimeric receptor. Here we describe our investigation of the potential role of IL-21 in hematopoiesis.

2. Materials and Methods

2.1. Cytokines and Cell Culture

All cytokines were from R&D Systems (Minneapolis, MN, USA). Cells were cultured in RPMI 1640 complete

Correspondence and reprint requests: Katsutoshi Ozaki, MD, PhD, Division of Hematology, Jichi Medical University, 3311-1 Yakushiji, Shimotsuke-shi, Tochigi 329-0498, Japan; 81-285-58-7353; fax: 81-285-44-5258 (e-mail: ozakikat@jichi.ac.jp).

medium (Sigma-Aldrich, St. Louis, MO, USA) supplemented with 10% heat-inactivated fetal bovine serum, sodium pyruvate, nonessential amino acids, and penicillin-streptomycin (Invitrogen/Life Technologies, Rockville, MD, USA).

2.2. Mice

C57BL/6J (CD45.2) and congenic C57BL/6-Ly5.1 (CD45.1) were from CLEA Japan (Tokyo, Japan) and Sankyo Laboratory (Tokyo, Japan), respectively. $RAG2^{-/-}$ mice were a kind gift from Dr. Satoshi Takaki (The University of Tokyo).

2.3. Bone Marrow Mononuclear Cell Preparation

5-Fluorouracil (5-FU) (Sigma-Aldrich) at 150 mg/kg was administered via intraperitoneal injection. Three or four days later, the mice were sacrificed, and femurs and tibias were excised and flushed. If necessary, mononuclear cells were isolated with Lymphoprep (Axis-Shield, Oslo, Norway).

2.4. Splenocyte Preparation

Spleens were crushed with nylon mesh in erythrocyte-lysis buffer (ACK buffer: 8.29 g NH_4Cl, 1.00 g $KHCO_3$, and 0.0372 g EDTA in 1 L). After the addition of medium and centrifugation, splenocytes were counted and used for the colony-forming unit (CFU) assay and fluorescence-activated cell-sorting (FACS) analysis.

2.5. CFU Assay

For the CFU–granulocyte-macrophage (CFU-GM) assay, we used methylcellulose containing IL-3, IL-6, and stem cell factor (SCF) (M3534; StemCell Technologies, Vancouver, British Columbia, Canada). For the CFU-granulocyte (CFU-G), CFU-macrophage (CFU-M), CFU-GM, burst-forming unit–erythroid (BFU-E), and CFU–granulocyte, erythrocyte, megakaryocyte, macrophage (CFU-GEMM) assays, we used methylcellulose containing IL-3, IL-6, SCF, and erythropoietin (M3434; StemCell Technologies).

2.6. Peripheral Blood Cell Preparation

For FACS analysis, blood was collected, lysed with erythrocyte-lysis buffer, and analyzed. Complete blood counts were determined with an automated counter (Sysmex Corporation, Tokyo, Japan).

2.7. Flow Cytometric Analysis

Fc Block (blocking antibody against CD16 and CD32; BD Biosciences, San Jose, CA, USA) was used to eliminate nonspecific binding of the antibody to Fc receptors. Propidium iodide at 5 μg/mL was added to gate out dead cells. Antibodies conjugated with fluorescein isothiocyanate (FITC), phycoerythrin (PE), or allophycocyanin were used for analysis on a FACSCalibur flow cytometer (BD Medical Systems, Franklin Lakes, NJ, USA). All antibodies were from BD Pharmingen (San Diego, CA, USA) or eBioscience (San Diego, CA, USA), except for the biotin-conjugated antibodies, which were components of a Lineage Cell Depletion kit from Miltenyi Biotec (Auburn, CA, USA).

2.8. IL-21 Overexpression In Vivo

Murine IL-21 complementary DNA was subcloned into a pORF expression vector (InvivoGen, San Diego, CA, USA), and an empty pORF expression vector was used as a negative control. Briefly, 20 μg of the empty vector or the IL-21 vector in 2 mL phosphate-buffered saline was administered intravenously into the tail vein, as previously described [7,8]. This method of protein expression in vivo is known as hydrodynamics-based transfection [13,14].

2.9. Cell Sorting

Bone marrow (BM) and spleen cells were stained with antibodies as described above and sorted with a FACSVantage instrument (BD Medical Systems). We first depleted differentiated cells with a Lineage Cell Depletion kit containing biotin-conjugated antibodies for CD5, B220, CD11b, Gr-1, 7-4, and Ter-119 (Miltenyi Biotec), stained them with FITC–Sca-1, PE–c-Kit, and lineage marker again, and sorted them for c-Kit^+ and Sca-1^+ double-positive cells with a gating out of the $lineage^+$ cells.

2.10. Reverse Transcriptase–Polymerase Chain Reaction Analysis

Total RNA or polyA RNA was obtained from sorted cells, KSL cells (c-Kit^+, Sca-1^+, and $lineage^{-/low}$ cells), cells positive for both Gr-1 and Mac-1, $B220^+$ cells, and $CD3^+$ cells by using RNAeasy (Qiagen, Valencia, CA, USA) or QuickPrep (GE Healthcare, Piscataway, NJ, USA). Glyceraldehyde phosphate dehydrogenase (GAPDH) was used as a loading control. Briefly, after the amount of GAPDH RNA was measured by reverse transcriptase–polymerase chain reaction (RT-PCR) analysis, the same amount of RNA was subjected to RT-PCR for the IL-21R. The primers used were as follows: GAPDH, 5′-CTCAACTAC ATGGTTTACATGTTCC-3′ and 5′-GCCAGTGGACTC CACGACGTAC-3′; IL-21R, 5′-ATGCCCCGGGGCCCA GTGGCTG-3′ and 5′-CACAGCATAGGGGTCTCTGAG GTTC-3′; ANG-1, 5′-CAGTGGCTGCAAAAACTTGA-3′ and 5′-ACGAGAAACCAAGCCTTGAA-3′.

2.11. BM Transplantation

Unless otherwise stated, recipient mice were irradiated with 9.50 Gy by means of an x-ray irradiation machine (Hitachi, Tokyo, Japan). Donor cells were injected into the tail vein.

2.12. Competitive Repopulation Assay

One thousand BM KSL cells from a Ly5.1 mouse with 2.5×10^5 Ly5.2 BM cells were injected into irradiated C57BL6/J mice. Repopulation of the peripheral blood was assessed by using antibodies to CD45.1 and/or lineage markers.

Table 1.
Flow Cytometric Analysis of Splenocytes and Peripheral Blood Cells from Control and Interleukin 21 (IL-21)-Overexpressing Mice*

	pORF, %	mIL-21/pORF, %
Spleen		
Sca-1	39.38 ± 3.01	62.41 ± 4.42†
c-Kit	2.53 ± 0.89	3.76 ± 1.17
CD11b	8.91 ± 2.11	9.87 ± 1.34
Gr-1	2.5 ± 1.39	2.28 ± 0.25
Ter-119	9.98 ± 3.21	16.52 ± 2.9
Peripheral blood		
Sca-1	36.33 ± 1.71	62.57 ± 3.61†
c-Kit	0.13 ± 0.02	0.16 ± 0.05
CD11b	18.13 ± 1.91	24.31 ± 1.10†
Gr-1	7.11 ± 2.27	7.96 ± 0.84

*Data are expressed as the percentage of cells expressing the indicated marker and are presented as the mean ± SD. pORF indicates mice injected with empty pORF expression vector; mIL-21/pORF, mice injected with pORF vector expressing the murine IL-21 gene.
†$P < .05$, Student t test.

2.13. Enzyme-Linked Immunosorbent Assay for IL-21

A mouse IL-21 enzyme-linked immunosorbent assay kit was purchased from R&D Systems and used per the manufacturer's instructions.

2.14. Statistical Analysis

We used the Student t test for the determination of P values. A P value of <.05 was considered statistically significant.

3. Results

3.1. IL-21 Increases Sca-1$^+$ Cells in the Spleen and Peripheral Blood

Previously, we used a hydrodynamics-based transfection method [13,14] to establish an in vivo system of transient IL-21 overexpression [8], which resulted in serum IL-21 concentrations as high as 6 ng/mL for a period of several days [8]. The primary site of expression has been reported to be the hepatocyte [14], and the secreted IL-21 most likely circulates in the blood. Spleens from mice overexpressing IL-21 were larger than the spleens of control mice and contained 1.5- to 2.0-fold more cells [7]. This larger spleen size and the decreased expression of CD21 and CD23 on B-cells [7] were used as markers for IL-21 overexpression. Using the same system in the present study, we observed an increased percentage of Sca-1$^+$ cells in the spleen and peripheral blood (Table 1). In these particular experiments, the concentration of murine IL-21 in the sera of mice injected with murine IL-21 vector was 494 ± 360 pg/mL (mean ± SD; n = 6) at day 6, whereas the concentration of murine IL-21 in sera from mice injected with empty vector was, as expected, at approximately the lower limit of detection (24 ± 4 pg/mL; n = 6).

3.2. IL-21 Increases CFU-GM in the Spleen

What does an increase of Sca-1$^+$ cells in the spleen imply? Because Sca-1 is a hematopoietic stem/progenitor cell marker, we performed CFU-GM assays with BM and spleen cells. The number of CFU-GM per spleen increased approximately 5-fold, whereas the increase in the CFU-GM in the femur (BM) did not achieve statistical significance (Figure 1A), indicating IL-21 induction of progenitor cell expansion in the spleen. To investigate what kinds of progenitors increased, we evaluated the numbers of CFU-G, CFU-M, CFU-GM, BFU-E, and CFU-GEMM. The main increase was in granulocyte-macrophage lineages in the spleen (Figure 1B).

3.3. IL-21 Increases KSL Cells in BM and Spleen

The increases in CFU-GM and Sca-1$^+$ cells in the spleen led us to investigate whether there was an increase in the phenotypic hematopoietic stem cell compartment, as defined by KSL cells in the BM and spleen. The percentages of KSL cells in the BM and spleen were induced by IL-21 (Figure 1C: ii versus i; iv versus iii). The cellularity in the spleen increased, whereas that in the BM either did not change or slightly decreased, resulting in a dramatic increase in total KSL cells in the spleen (Figure 1C, vi) and a more modest increase in total KSL cells in the BM (Figure 1C, v).

3.4. IL-21 Augments Proliferation of KSL Cells In Vitro

We next assessed whether IL-21 augments the proliferation of hematopoietic stem cells in vitro. We used a combination of murine SCF (c-Kit ligand), human Flt-3 ligand (Flt-3L), and murine IL-7 as a cytokine "cocktail." BM cells from 5-FU–treated mice were incubated with the cytokine cocktail for 1 week in the presence or absence of IL-21. The total number of BM cells was greater when IL-21 was added (Figure 2A, upper panel). To eliminate any effects from differentiated cells, we used sorted KSL cells from untreated BM cells instead of 5-FU–treated BM cells. From 1000 KSL cells, cells treated with IL-21 increased to 30,000 cells after 1 week, but cells without IL-21 treatment expanded to only 10,000 cells (Figure 2A, lower panel). Regardless of the presence or absence of IL-21, KSL cells gave rise to B-lymphoid and myeloid cells, according to the results of B220, Mac-1, and Gr-1 staining. These results suggest that IL-21 was able to augment the proliferation of hematopoietic progenitor cells, at least in the presence of SCF, Flt-3L, and IL-7.

3.5. KSL Cells Express IL-21R

Given that IL-21 augments the proliferation of KSL cells, KSL cells should express IL-21R. To determine if KSL cells express IL-21R, we used semiquantitative RT-PCR analysis for KSL cells, Gr-1$^+$Mac-1$^+$ BM cells, B220$^+$ spleen cells, and CD3$^+$ spleen cells. IL-21R was expressed on KSL cells but at a lower level than on T-cells and B-cells (Figure 2B). Five independently sorted KSL cell preparations demonstrated IL-21R expression, as confirmed by DNA sequencing of the PCR fragments. Gr-1$^+$Mac-1$^+$ cells from

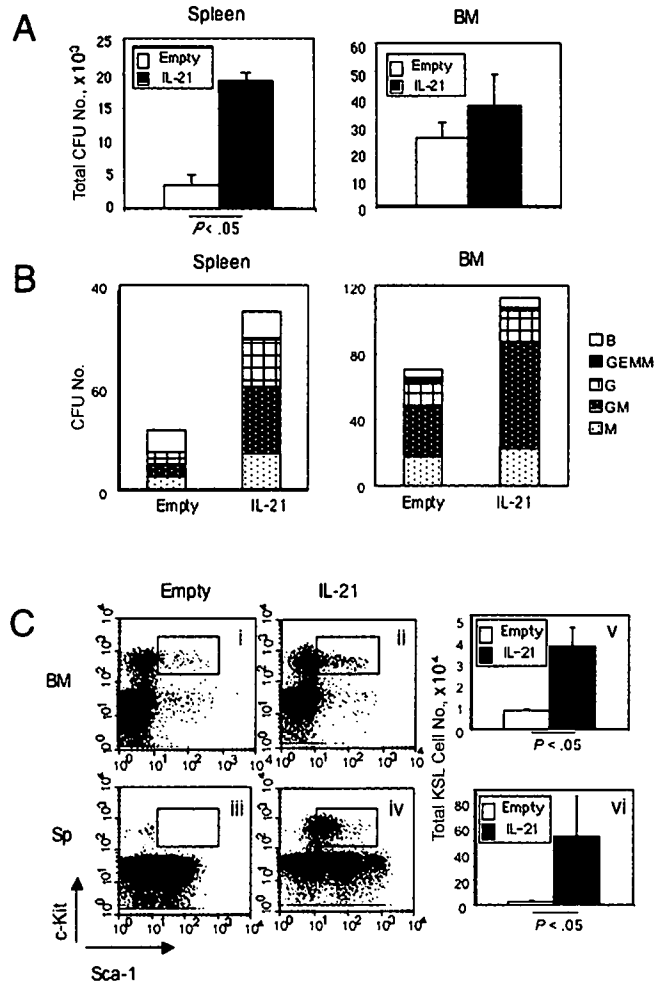

Figure 1. Numbers of colony-forming units (CFU) and c-Kit$^+$, Sca-1$^+$, and lineage$^{-/low}$ (KSL) cells in bone marrow (BM) and spleen (Sp). A, Evaluation of CFU–granulocyte-macrophage (CFU-GM). Splenocytes (2.5×10^5 cells) or BM cells (5×10^4 cells) were plated in methylcellulose medium (MethoCult GF M3534) containing interleukin 3 (IL-3), IL-6, and stem cell factor (SCF) (StemCell Technologies). The numbers of colonies were counted after 5 to 7 days and expressed as the number of CFU-GM per spleen or femur (BM). Data are expressed as the mean ± SD for 3 mice in each group, and the data presented are representative of more than 3 independent experiments. B, Evaluation of CFU-granulocyte (G), CFU-macrophage (M), CFU-GM (GM), burst-forming unit–erythroid (B), and CFU–granulocyte, erythrocyte, megakaryocyte, macrophage (GEMM). Splenocytes (2.5×10^5 cells) or BM cells (5×10^4 cells) were plated in methylcellulose medium (MethoCult GF M3434) containing IL-3, IL-6, SCF, and erythropoietin (StemCell Technologies), and the numbers of colonies were counted after 5 to 7 days. The data are presented as the mean of 5 mice in each group. C, Overexpression of IL-21 increases the number of KSL cells. Typical KSL staining of BM cells (i, ii) and splenocytes (iii, iv) from mice injected with either empty vector or IL-21–expression plasmid, and the numbers of KSL cells in a femur (BM) (v) or spleen (vi). The result shown is a representative result from 2 independent experiments with 5 mice in each group. The difference is partly due to the elevated expression of Sca-1, as shown in Table 1, but is not due to the compensation conditions, because these mice were compared at the same time, with the same machine, and under identical conditions.

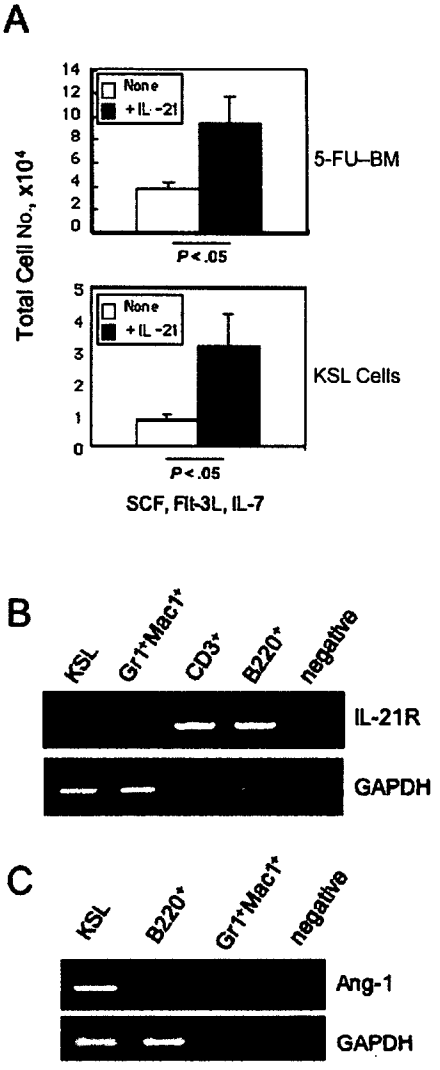

Figure 2. Augmentation of c-Kit$^+$, Sca-1$^+$, and lineage$^{-/low}$ (KSL) cell proliferation Interleukin 21 (IL-21) and expression of IL-21 receptor (IL-21R) on KSL cells. A, Total cell numbers after incubation with or without IL-21 using 5-fluorouracil–treated bone marrow cells (5-FU–BM) (upper panel) or purified KSL cells from untreated BM (lower panel). BM mononuclear cells (1×10^6) from 5-FU–treated mice or 1000 sorted BM KSL cells were incubated in a cytokine cocktail (20 ng/mL murine stem cell factor [SCF], 20 ng/mL human Flt-3 ligand [Flt-3L], and 50 ng/mL murine IL-7) with or without murine IL-21 (20 ng/mL), and cell numbers were counted after 1 week. We cultured cells under normal conditions and used no supporting cell lines, such as stromal cells. Shown is a representative result from 2 independent experiments. Error bars represent the SD of triplicate measurements. B, Semiquantitative reverse transcriptase–polymerase chain reaction (RT-PCR) analysis of IL-21R. Glyceraldehyde phosphate dehydrogenase (GAPDH) was used as a loading control. The same amount of RNA was subjected to the RT-PCR for IL-21R. Shown is a representative result from 5 independently sorted KSL cell populations. C, RT-PCR analysis of Ang-1, which has been reported to be expressed on hematopoietic stem cells as well as on stromal cells [15]. GAPDH was used as a loading control. The same amount of RNA was subjected to the RT-PCR for Ang-1.

the BM did not express IL-21R messenger RNA, suggesting that differentiated myeloid cells in the BM do not express IL-21R or that the expression level is diminished. Even though cell purity after sorting was >98%, we verified the cell quality further by checking the expression of Ang-1 (the ligand for the Tie-2 receptor), which is known to be expressed on hematopoietic stem cells [15] as well as stromal cells and which is critical for angiogenesis [15]. Among the cell populations we examined, only KSL cells expressed Ang-1 (Figure 2C).

3.6. IL-21 Also Increases CFU-GM and KSL Cells in RAG2$^{-/-}$ Mice

There are 2 possible mechanisms, a direct mechanism and an indirect mechanism, for the effect of IL-21 on the expansion of progenitor cells. To date, the cells known to express IL-21R are T-cells, B-cells, NK cells, and dendritic cells. In terms of cell numbers, NK and dendritic cells are much less abundant than mature T-cells and B-cells. To investigate the possibility of a secondary effect from mature T-cells and B-cells, we used RAG2 knock-out mice, which lack mature T-cells and B-cells. In these mice, IL-21 overexpression induced a dramatic increase of KSL cells in the spleen (Figure 3A: iv versus iii; vi), a more modest increase of KSL cells in the BM (Figure 3A: ii versus i; v), and a corresponding increase of CFU-GM in the spleen (Figure 3B), analogous to results for normal mice. Thus, mature T-cells and B-cells are not required for the increase in KSL cells and CFU-GM induced by IL-21. The degree of induction in the number of KSL cells by IL-21 in normal mice is much greater than that in the number of CFU-GM (Figure 1C [v and vi] versus Figure 1A), but the difference in the magnitudes of the inductions is not as evident in RAG2$^{-/-}$ mice (Figure 3A [v and vi] versus Figure 3B), suggesting that secondary signals from mature T-cells and B-cells augment the increase in KSL cells but not in CFU-GM. Previously, we confirmed that IL-21 overexpression did not induce an elevation in the serum levels of various cytokines, including IL-1β, IL-2, IL-4, IL-5, IL-12, and tumor necrosis factor α [8]. Consistent with this result, no IL-21–induced elevation of interferon γ, granulocyte-macrophage colony-stimulating factor (GM-CSF), or IL-4 has been demonstrated [9]. These results suggest a direct rather than an indirect effect of IL-21; however, we could not exclude the possible contribution of dendritic, NK, or other unknown cells to the expansion of hematopoietic progenitor cells induced by IL-21.

3.7. Spleen KSL Cells Increased by IL-21 in Wild-Type Mice Have Less CFU-GM Activity than BM KSL Cells

The result with RAG2$^{-/-}$ mice suggests that mature T-cells and B-cells are responsible for the further increase in KSL cells in wild-type mice. The additional degree of induction in KSL cells but not in CFU-GM suggests the presence of less functional KSL cells. To observe the relationship between the induced KSL cells and CFU-GM numbers directly, we performed a CFU-GM assay with the same numbers of sorted

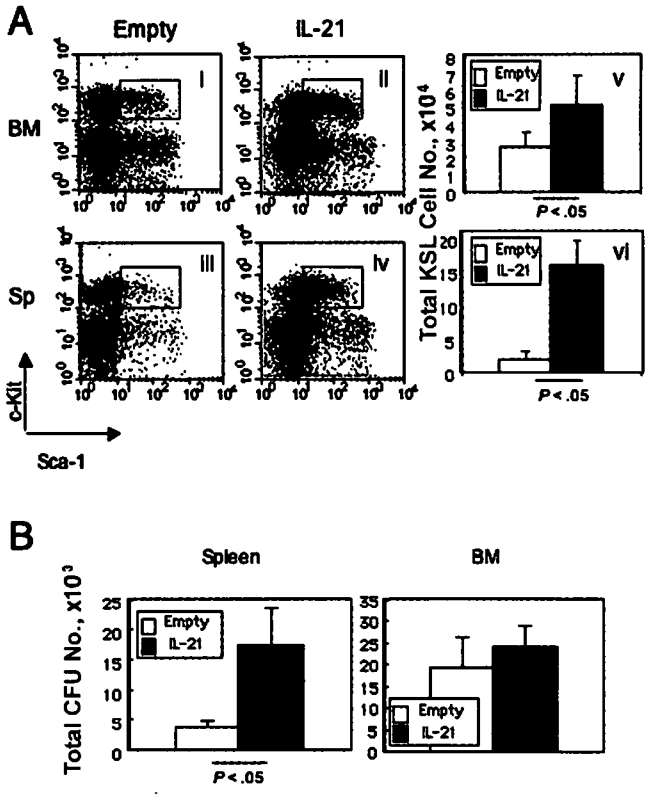

Figure 3. Interleukin 21 (IL-21) induces c-Kit$^+$, Sca-1$^+$, and lineage$^{-/low}$ (KSL) cells and colony-forming units–granulocyte-macrophage (CFU-GM) in RAG2$^{-/-}$ mice. A, KSL cell staining and the number of KSL cells. Typical KSL cell staining of bone marrow (BM) cells (i, ii) or splenocytes (Sp) (iii, iv) from RAG2$^{-/-}$ mice injected with either empty vector or IL-21 vector and the total number of KSL cells in a femur (BM) (v) or spleen (vi). The result shown is the combined results from 2 sets of 6 mice injected with either empty vector or IL-21 expression vector. Error bars indicate ±SD. The difference is partly due to the elevated expression of Sca-1, as shown in Table 1, but is not due to the compensation conditions, because these mice were compared at the same time, with the same machine, and under identical conditions. B, The number of CFU-GM in the spleen and BM (femur) from RAG2$^{-/-}$ mice injected with either empty vector or IL-21 vector. Shown is a combined result for 7 mice for each experimental condition. Error bars indicate ±SD.

KSL cells from wild-type mice injected with empty vector and mice injected with IL-21 vector. BM KSL cells from both types of mice yielded similar numbers of CFU-GM (Figure 4A, left and middle bars). The increased spleen KSL cells also formed CFU-GM colonies (Figure 4A, right bar), but the frequency was lower than in the BM KSL cells, suggesting that the increased splenic KSL cells have less colony-forming activity than BM KSL cells. These results account for the discrepancy in the magnitudes of the inductions between the CFU-GM and KSL cells in the spleen but not in the BM.

Next, we transplanted 1000 BM KSL cells and found that the reconstitution abilities after 3 months for BM KSL cells from the 2 types of mice were indistinguishable (Figure 4B). However, reconstitution after 1 month was lower in mice injected with BM KSL cells induced by IL-21, suggesting that

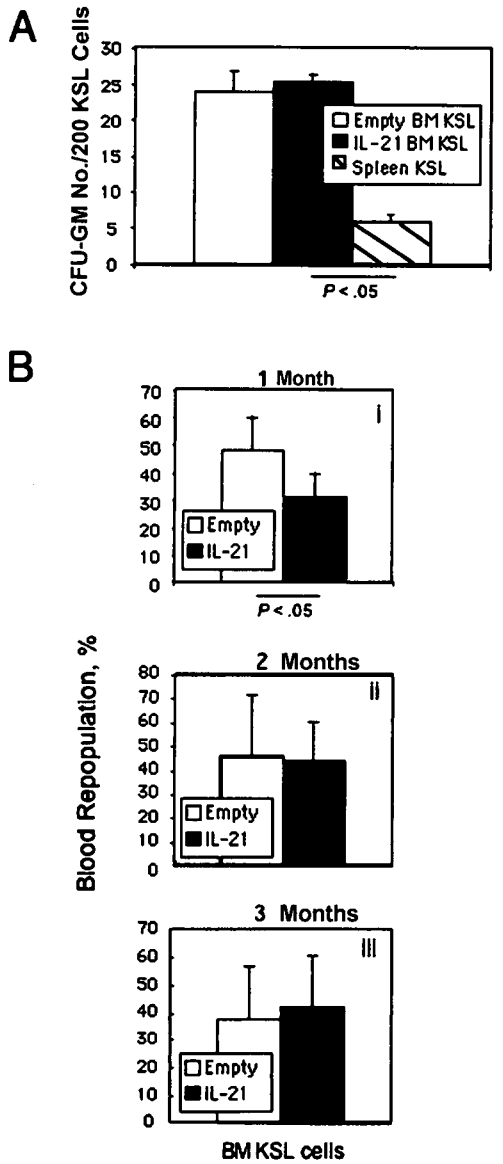

Figure 4. Analysis of induced c-Kit$^+$, Sca-1$^+$, and lineage$^{-/low}$ (KSL) cells. A, The number of colony-forming units–granulocyte-macrophage (CFU-GM) from 1000 bone marrow (BM) KSL cells from mice injected with either empty vector or IL-21 vector and from 1000 spleen KSL cells from mice injected with IL-21 vector. Shown is a representative result from 2 independent experiments. Six mice from each treatment were analyzed. B, Competitive repopulation analysis of the induced BM KSL cells. One thousand BM KSL cells from mice injected with either empty vector or IL-21 vector were transplanted, and peripheral blood engraftment was analyzed according to the percentage of CD45.1$^+$ cells after 1 (i), 2 (ii), and 3 (iii) months. Shown is a representative result from 2 independent experiments. Eight mice from each treatment were analyzed. Error bars indicate ± SD.

BM KSL cells sorted from mice injected with the IL-21 vector contain equal numbers of long-term hematopoietic stem cells but fewer short-term hematopoietic stem cells, compared with BM KSL cells sorted from the mice injected with the control vector.

4. Discussion

We report that overexpression of IL-21 induces an expansion of hematopoietic progenitor cells in the spleen. To our knowledge, this report is the first to show that IL-21 affects hematopoiesis in vivo by either a direct or an indirect mechanism. KSL cells express IL-21R, but the level of expression is low. Further experiments are needed to determine whether this expression is functional, which components of the stem cell compartment express this receptor, and whether a direct or an indirect effect of IL-21 induces the expansion of hematopoietic progenitor cells. We hypothesize that IL-21 has a costimulatory effect on progenitor cell proliferation in the presence of other cytokines, similar to the effect of IL-21 on T-cells or NK cells [1].

We have reported that overexpression of IL-21 induces an increase in immature B-cells [11] in the spleen, although the molecular mechanism remains unknown. The results reported here suggest that this increase might be derived from the induction of progenitor cells in the spleen. It is interesting that human IL-6/soluble human IL-6R double-transgenic mice, but not human IL-6 transgenic mice, exhibit extramedullary hematopoiesis and show elevated numbers of KSL cells, CFU-GM, granulocytes, macrophages, and Sca-1$^+$ cells in the spleen [16], similar to results of our mice overexpressing IL-21. These double-transgenic mice do not exhibit an increase of peripheral white blood cells until 8 weeks of age [16]. An overall similar phenotype suggests that the cell population on which IL-21 and IL-6/soluble IL-6R act may be the same or a closely similar population. In this regard, it is interesting that both IL-6 and IL-21 activate Stat3.

The transient overexpression of IL-21 induces the expansion of hematopoietic progenitor cells in the spleen but appears to be insufficient for the survival and differentiation of these cells into granulocytes or monocytes, because the number of white blood cells in the periphery did not increase. The lack of IL-21R expression on BM-derived myelomonocytes suggests that IL-21 is able to augment the proliferation of primitive cells but not differentiated myelomonocytes.

Overexpression of IL-21 in vivo induced CFU-GM in the spleen (Figures 1A and 1B) and reduced short-term hematopoietic stem cells in the BM (Figure 4B, i), suggesting that the simplest explanation for this phenomenon is a conversion of short-term hematopoietic stem cells into more differentiated colony-forming cells. More detailed experiments are needed to establish evidence for this hypothesis.

A discrepancy between the increases in KSL cells and CFU-GM occurred only in wild-type mice. The presence of less functional "phenotypic" KSL cells in the spleen accounts for the discrepancy between the increases in KSL cells and CFU-GM in the spleen (Figure 4A). In the case of BM, in contrast to the spleen, we could not explain the discrepancy by the less functional "phenotypic" KSL cells (Figure 4A). However, in the absence of mature T-cells and B-cells, the discrepancy disappeared (Figure 3), suggesting that these discrepancies are due to modification by secondary signals from mature T-cells and B-cells and are not a direct effect of IL-21.

CD34$^-$ KSL cells have been demonstrated to express γc [12]. Recently, the hematopoietic hierarchy has been determined, and the expression of γc was reported to be progres-

sively up-regulated from hematopoietic stem cells to committed lymphoid progenitors to pro–T-cells [17]. These reports provide supporting evidence that the presence of the IL-21R on hematopoietic stem/progenitor cells enables them to respond to IL-21 stimulation.

From investigations of IL-21R–deficient mice, it is clear that IL-21 is dispensable for hematopoiesis under normal conditions [5,6]. Our data nevertheless suggest that IL-21 might contribute to hematopoiesis in a redundant fashion and moreover suggest that IL-21 could be useful in inducing differentiated hematopoietic cells in combination with another, yet undetermined cytokine, such as G-CSF, GM-CSF, or IL-7. In such a combination, IL-21 could have potentially therapeutic uses related to its ability to promote the expansion of hematopoietic progenitor cells.

Acknowledgments

This work was supported by a grant from the Chugai Pharmaceutical Company. The research was supported in part by the Intramural Research Program of the National Heart, Lung, and Blood Institute, National Institutes of Health, Bethesda, Maryland, USA. We thank Dr. Satoshi Takaki for providing RAG2$^{-/-}$ mice.

References

1. Parrish-Novak J, Dillon SR, Nelson A, et al. Interleukin 21 and its receptor are involved in NK cell expansion and regulation of lymphocyte function. *Nature*. 2000;408:57-63.
2. Ozaki K, Kikly K, Michalovich D, Young PR, Leonard WJ. Cloning of a type I cytokine receptor most related to the IL-2 receptor β chain. *Proc Natl Acad Sci U S A*. 2000;97:11439-11444.
3. Asao H, Okuyama C, Kumaki S, et al. Cutting edge: the common γ-chain is an indispensable subunit of the IL-21 receptor complex. *J Immunol*. 2001;167:1-5.
4. Habib T, Senadheera S, Weinberg K, Kaushansky K. The common γ chain (γc) is a required signaling component of the IL-21 receptor and supports IL-21-induced cell proliferation via JAK3. *Biochemistry*. 2002;41:8725-8731.
5. Kasaian MT, Whitters MJ, Carter LL, et al. IL-21 limits NK cell responses and promotes antigen-specific T cell activation: a mediator of the transition from innate to adaptive immunity. *Immunity*. 2002;16:559-569.
6. Ozaki K, Spolski R, Feng CG, et al. A critical role for IL-21 in regulating immunoglobulin production. *Science*. 2002;298:1630-1634.
7. Ozaki K, Spolski R, Ettinger R, et al. Regulation of B cell differentiation and plasma cell generation by IL-21, a novel inducer of Blimp-1 and Bcl-6. *J Immunol*. 2004;173:5361-5371.
8. Wang G, Tschoi M, Spolski R, et al. In vivo antitumor activity of interleukin 21 mediated by natural killer cells. *Cancer Res*. 2003;63: 9016-9022.
9. Kishida T, Asada H, Itokawa Y, et al. Interleukin (IL)-21 and IL-15 genetic transfer synergistically augments therapeutic antitumor immunity and promotes regression of metastatic lymphoma. *Mol Ther*. 2003;8:552-558.
10. Zeng R, Spolski R, Finkelstein SE, et al. Synergy of IL-21 and IL-15 in regulating CD8$^+$ T-cell expansion and function. *J Exp Med*. 2005;201:139-148.
11. King C, Ilic A, Koelsch K, Sarvetnick N. Homeostatic expansion of T cells during immune insufficiency generates autoimmunity. *Cell*. 2004;117:265-277.
12. Nakauchi H, Takano H, Ema H, Osawa M. Further characterization of CD34-low/negative mouse hematopoietic stem cells. *Ann N Y Acad Sci*. 1999;872:57-66.
13. Liu F, Song Y, Liu D. Hydrodynamics-based transfection in animals by systemic administration of plasmid DNA. *Gene Ther*. 1999;6: 1258-1266.
14. Zhang G, Budker V, Wolff JA. High levels of foreign gene expression in hepatocytes after tail vein injections of naked plasmid DNA. *Hum Gene Ther*. 1999;10:1735-1737.
15. Takakura N, Watanabe T, Suenobu S, et al. A role for hematopoietic stem cells in promoting angiogenesis. *Cell*. 2000;102:199-209.
16. Peters M, Schirmacher P, Goldschmitt J, et al. Extramedullary expansion of hematopoietic progenitor cells in interleukin (IL)-6-sIL-6R double transgenic mice. *J Exp Med*. 1997;185:755-766.
17. Terskikh AV, Miyamoto T, Chang C, et al. Gene expression analysis of purified hematopoietic stem cells and committed progenitors. *Blood*. 2003;102:94-101.

Protection Against Aminoglycoside-induced Ototoxicity by Regulated AAV Vector–mediated GDNF Gene Transfer Into the Cochlea

Yuhe Liu[1,2,3], Takashi Okada[1,4], Kuniko Shimazaki[5], Kianoush Sheykholeslami[6], Tatsuya Nomoto[1], Shin-Ichi Muramatsu[7], Hiroaki Mizukami[1], Akihiro Kume[1], Shuifang Xiao[3], Keiichi Ichimura[2] and Keiya Ozawa[1]

[1]Division of Genetic Therapeutics, Jichi Medical University, Tochigi, Japan; [2]Department of Otolaryngology, Jichi Medical University, Tochigi, Japan; [3]Department of Otolaryngology, Peking University First Hospital, Beijing, China; [4]Department of Molecular Therapy, National Institute of Neuroscience, National Center of Neurology and Psychiatry, Tokyo, Japan; [5]Department of Physiology, Jichi Medical University, Tochigi, Japan; [6]Department of Neurobiology, Northeastern Ohio Universities College of Medicine, Rootstown, Ohio, USA; [7]Division of Neurology, Department of Medicine, Jichi Medical University, Tochigi, Japan

Since standard aminoglycoside treatment progressively causes hearing disturbance with hair cell degeneration, systemic use of the drugs is limited. Adeno-associated virus (AAV)-based vectors have been of great interest because they mediate stable transgene expression in a variety of postmitotic cells with minimal toxicity. In this study, we investigated the effects of regulated AAV1-mediated glial cell line–derived neurotrophic factor (GDNF) expression in the cochlea on aminoglycoside-induced damage. AAV1-based vectors encoding GDNF or vectors encoding GDNF with an rtTA2s-S2 Tet-on regulation system were directly microinjected into the rat cochleae through the round window at 5×10^{10} genome copies/body. Seven days after the virus injection, a dose of 333 mg/kg of kanamycin was subcutaneously given twice daily for 12 consecutive days. GDNF expression in the cochlea was confirmed and successfully modulated by the Tet-on system. Monitoring of the auditory brain stem response revealed an improvement of cochlear function after GDNF transduction over the frequencies tested. Damaged spiral ganglion cells and hair cells were significantly reduced by GDNF expression. Our results suggest that AAV1-mediated expression of GDNF using a regulated expression system in the cochlea is a promising strategy to protect the cochlea from aminoglycoside-induced damage.

Received 12 May 2007; accepted 15 November 2007; published online 8 January 2008. doi:10.1038/sj.mt.6300379

INTRODUCTION

Aminoglycoside antibiotics are frequently used in empiric therapy for serious infections, such as septicemia, complicated intra-abdominal infections, complicated urinary tract infections, and nosocomial respiratory tract infections. However, it is well known that aminoglycosides are associated with severe side effects, such as ototoxicity and nephrotoxicity, which attack the cochlea or vestibule and destroys the auditory and vestibular hair cells that pass information to the auditory nerve.[1] In addition, aminoglycosides predominantly destroy the outer hair cells by ototoxicity. Although the exact mechanism of damage is not well established,[2] aminoglycoside-induced hair cell loss results in a permanent hearing deficit[3] that can progressively occur 6 months to a year after exposure to these drugs. Therefore, the development of a strategy to prevent aminoglycoside-associated ototoxicity before adverse events occur is a critical issue in clinical settings.

The expression of a transgene using viral vectors is a potential approach to introduce neurotrophic factors into the cochlea to prevent and treat aminoglycoside-induced hearing loss. However, most of the currently used vectors, such as adenovirus vectors or herpes simplex virus vectors, have an associated vector-related cytotoxicity.[4,5] Hence, adeno-associated virus (AAV) vectors may be good candidates for gene transfer into the cochlear cells because of their efficient transduction and their safety and potential in long-term expression.[6] We have previously demonstrated that an AAV1-based vector efficiently transduced the inner hair cells, the spiral ganglion cells, and many other types of cells.[7] Therefore, an AAV1-based vector should successfully introduce secretory proteins, such as glial cell line–derived neurotrophic factor (GDNF), into the cochlea to prevent aminoglycoside-induced ototoxicity.

GDNF, a member of the transforming growth factor β family, was initially identified as a survival factor for mid-brain dopaminergic neurons and for a wide range of neuronal populations in the central and peripheral nervous systems.[8–10] Although it is still unclear whether GDNF protects against ototoxicity, sustained infusion of recombinant GDNF protected the cochlear structure and function from noise- and drug-induced damage and stress,[11–18] although its half-life is very short. However, an overdose of GDNF was shown to enhance the sensitivity of the cochleae to insult and

Correspondence: *Takashi Okada, Department of Molecular Therapy, National Institute of Neuroscience, National Center of Neurology and Psychiatry, 4-1-1 Ogawa-Higashi, Kodaira, Tokyo 187-8551, Japan. E-mail: t-okada@ncnp.go.jp; Keiya Ozawa, Division of Genetic Therapeutics, Center for Molecular Medicine, Jichi Medical University, 3311-1 Yakushiji, Shimotsuke, Tochigi 329-0498, Japan. E-mail: kozawa@jichi.ac.jp*

to destroy cochlear function.[12] Furthermore, it has been reported that testicular tumors are formed in GDNF-overexpressing mice.[19] Therefore, an appropriate regulation system is required to realize the therapeutic benefits of GDNF expression.

Regulated transgene expression has been successfully achieved in various gene therapy experiments using the Tet system.[20–23] Notably, tetracycline derivatives, such as doxycycline (Dox), activate the Tet-on system at doses 100-fold lower than tetracycline. Furthermore, the reverse Tet-responsive transcriptional activator (rtTA) series were improved through the generation of variants called rtTA2s-S2, which showed lower leakiness and better inducibility in HeLa cells and mice.[24,25]

In this study, we describe *in vivo* therapeutic experiments utilizing AAV1 vector–mediated tetracycline-regulated expression of GDNF in cochleae. We demonstrate that AAV1 vector–mediated GDNF expression protects sensory cells in the inner ear from drug-induced degeneration.

RESULTS

Expression and distribution of transgene in the cochlea

AAV1-EGFP or AAV1-GDNF containing either the enhanced humanized green fluorescent protein (*EGFP*) gene or the *GDNF* gene under the control of the CAG (human cytomegalovirus (CMV) immediate-early enhancer and Chicken β-actin promoter) promoter, and the Woodchuck hepatitis virus posttranscriptional regulatory element (WPRE) (**Figure 1a**), was injected into the cochlea. The GDNF protein level in the perilymph was measured by enzyme-linked immunosorbent assay (**Figure 2a**). There was a significant increase in GDNF concentration in the cochlea transduced with AAV1-GDNF. The widespread distribution of the GDNF expression was observed in the cochlea, including the spiral ganglion and the inner hair cells (**Figure 2b**).

To examine the possible transduction of the contralateral ear with the virus diffusion, we analyzed the AAV vector–meditated transgene expression of the rodents with this transduction approach using the optical bioluminescence imaging. Luciferase expression was mainly detected at the injected side of the cochleae (5,370.3 photons/sec/cm²/sr, **Supplementary Figure S1**). Interestingly, the AAV vector also transduced the contralateral ear (876.8 photons/sec/cm²/sr), along with the brain (792.9 photons/sec/cm²/sr). Similar results were obtained with repeated experiments.

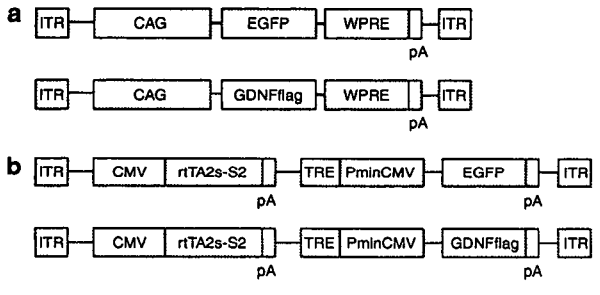

Figure 1 Schematic representation of the viral vectors used in this study. (**a**) An adeno-associated virus 1 (AAV1)-based vector was constructed using the CAG promoter to drive enhanced green fluorescent protein (EGFP) or mouse glial cell line–derived neurotrophic factor (GDNF) with a FLAG tag (GDNFflag). The Woodchuck hepatitis virus posttranscriptional regulatory element (WPRE) was inserted into the 3′ end of the transgene cassette. (**b**) The transactivator rtTA2s-S2 is under the control of the CMV promoter. The minimal CMV promoter (PminCMV) induces transgene expression (EGFP or GDNFflag) in combination with the Tetracycline-responsive element (TRE) and transactivator. CAG, human cytomegalovirus immediate-early enhancer and Chicken β-actin promoter; CMV, cytomegalovirus immediate-early promoter; pA, the simian virus 40 polyadenylation sequences; ITR, inverted terminal repeat from AAV2.

Preservation of the hair cells and spiral ganglion cells in the cochlea

Hair cell loss in the whole-mount cochleae of all the tested rat groups was analyzed by F-actin staining with rhodamine–phalloidin. **Figure 3a** shows a representative dissection through the second turn of the rat cochlea, in which a full complement of hair cells is revealed by F-actin phalloidin staining. In the vehicle-treated control group, outer hair cells in the base and middle turn were drastically lost after kanamycin treatment (**Figure 3b**). In the AAV1-GDNF/kanamycin-treated group, successful protection of the hair cells in the cochlea was observed (**Figure 3c**). In the contralateral cochlea, some of outer hair cells were also protected (**Figure 3d**). The spiral ganglion cell loss in the basal turn of the cochlea was assessed using 4′,6-diamino-2-phenylindole dihydrochloride staining (**Figure 4a** and **b**). Survival of the spiral ganglion cells in the AAV1-GDNF injected cochlea was significantly improved compared to that in the AAV1-EGFP injected cochlea (**Figure 4c**).

Protection of cochlear function by GDNF

Auditory brain stem response (ABR) recordings of the aminoglycoside-treated animals were performed to examine hearing

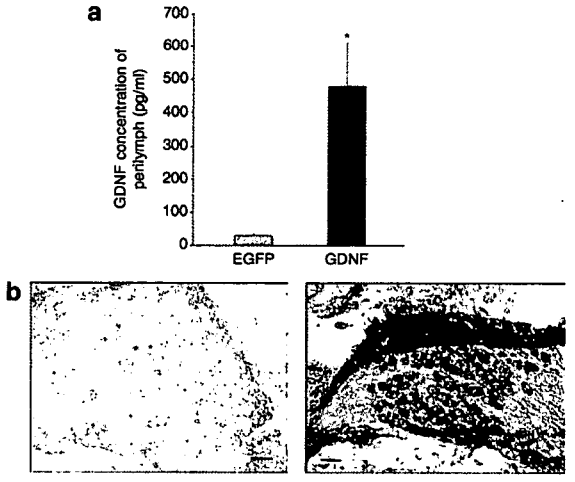

Figure 2 Expression and distribution of transgene in the cochlea. (**a**) Cochlear glial cell line–derived neurotrophic factor (GDNF) expression levels were measured by enzyme-linked immunosorbent assay in the transduced rats. GDNF expression level of the perilymph in the AAV1-GDNF/kanamycin group was significantly higher than that in the control group ($n = 5$, $P < 0.001$). (**b**) Immunohistochemistry was performed to analyze the expression of the GDNFflag in the rat cochlea. The AAV1-EGFP-transduced cochlea was used as a control (left). Cochlear sections were prepared after AAV1-GDNF injection and kanamycin administration. GDNflag expression was detected in the cochlea with an anti-FLAG antibody (right). Scale bar = 25μm; ×400. AAV1, adeno-associated virus 1; EGFP, enhanced green fluorescent protein.

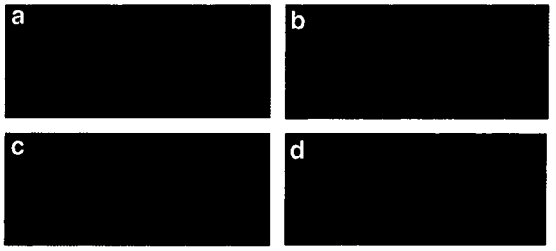

Figure 3 Preservation of the hair cells in the transduced cochlea. Hair cell loss in the cochlea of transduced rats was analyzed by F-actin staining. The dissected samples were dissected from the middle turn of the cochlea. The adeno-asssociated virus 1 (AAV1) vector was injected into the scala tympani of the cochlea prior to 12 days of kanamycin administration. (**a**) The normal cochlea. (**b**) The cochlea from the vehicle-treated ear; the many dark spaces represent the loss of outer hair cells. (**c**) The cochlea from the AAV1-GDNF-transduced ear. (**d**) The cochlea from the contralateral ear of AAV1-GDNF transduced rats. GDNF, glial cell line–derived neurotrophic factor.

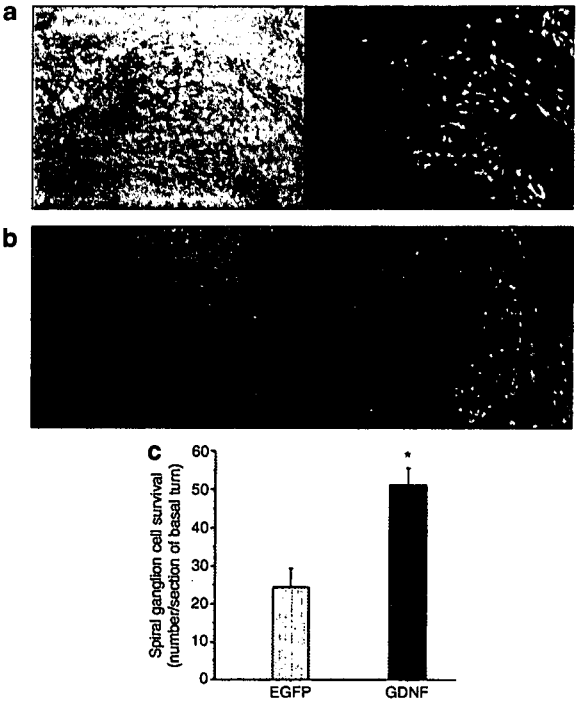

Figure 4 Survival of the spiral ganglion cells in the transduced cochlea. AAV1-GDNF-mediated rescue of the kanamycin-induced damage to the rat spiral ganglion neurons (SGNs): 4′,6-diamino-2-phenylindole dihydrochloride (DAPI) staining was performed on the sections obtained from the rat pretreated with either AAV1-EGFP or AAV1-GDNF, followed by kanamycin injections. (**a**, **b**) Representative photomicrographs of the cryosections showing the basal turn of the cochlear spiral (**a**, AAV1-EGFP; **b**, AAV1-GDNF). (**c**) The number of DAPI-positive large-nucleus cells that exhibited SGN morphology was counted. An asterisk denotes a statistically significant difference between the AAV1-GDNF and AAV1-EGFP-transduced rats (*t*-test, $P < 0.001$). AAV1, adeno-associated virus 1; EGFP, enhanced green fluorescent protein; glial cell line–derived neurotrophic factor.

impairment. At all frequencies tested, both GDNF-transduced and contralateral, untreated ears showed a significant improvement in the threshold shifts compared to the ears transduced with EGFP ($n = 5$, $P < 0.05$) (**Figure 5**). In the EGFP group, there was

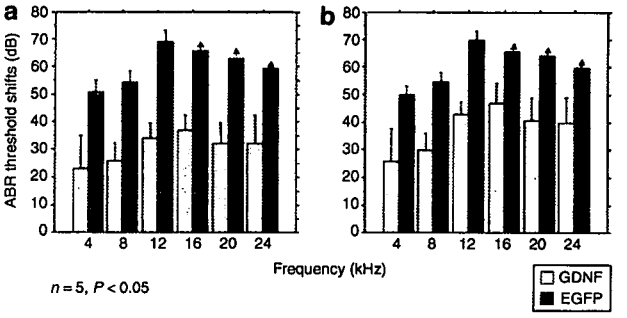

Figure 5 Protection of cochlear function by glial cell line–derived neurotrophic factor GDNF. Auditory brain stem response (ABR) threshold shifts (mean ± SD) of the (**a**) treated and (**b**) untreated ears at each tested frequency in the enhanced green fluorescent protein (EGFP) and GDNF transduced rats. The ABR threshold was measured twice in all the animals. The ears treated with AAV1-GDNF showed a significant improvement in the threshold shifts compared to the ears treated with AAV1-EGFP at all frequencies tested ($n = 5$, $P < 0.05$). Arrows indicate the average ABR thresholds that exceeded the output power of the ABR apparatus. AAV1, adeno-associated virus 1.

no significant difference in the ABR threshold shifts between the transduced and contralateral, untreated cochleae at all frequencies tested. Animals transduced with the AAV1-GDNF demonstrated lower ABR threshold shifts in the injected side compared to the contralateral side (at 12, 16, 20, 24 kHz; $P < 0.05$). These data indicate that both ears were protected even if the AAV1-GDNF was only injected into one ear.

Induced transgene expression

Two hundred and ninety three cells were transduced with the proviral plasmid harboring rtTA2s-S2 and the tetracycline-responsive element (TRE) to express the *EGFP* gene (**Figure 1b**). In the presence of Dox, a significant level of fluorescence was detected, suggesting that the rtTA2s-S2 system could switch on transcription following Dox treatment (**Figure 6a**). In contrast, reporter gene expression in the cultured cells was faint in the absence of Dox, indicating a low basal activity *in vitro*. Western blot analysis of GDNF showed that the transgene was induced in the presence of Dox, while no expression was detected in the absence of Dox (**Figure 6b**).

In vivo induction of GDNF expression and the dose–response to Dox

Enzyme-linked immunosorbent assay analysis of the GDNF expression level in muscle also showed low basal activity and induced expression after Dox treatment (**Figure 6c**). In the absence of Dox, the expression level of GDNF in the AAV2-S2-GDNF group was as low as that in the phosphate-buffered saline and AAV2-*LacZ* groups. On the other hand, significant increases in the GDNF level were observed in the muscle with increasing amounts of Dox, demonstrating that the rtTA2s-S2 system induces gene expression in a dose-dependent manner.

Inducible GDNF expression in the cochlea

Extensive inducible GDNF transgene expression was confirmed by immunohistochemistry using an anti-FLAG-antibody in the AAV1-S2-GDNF/kanamycin group in the presence of Dox (**Figure 7**).

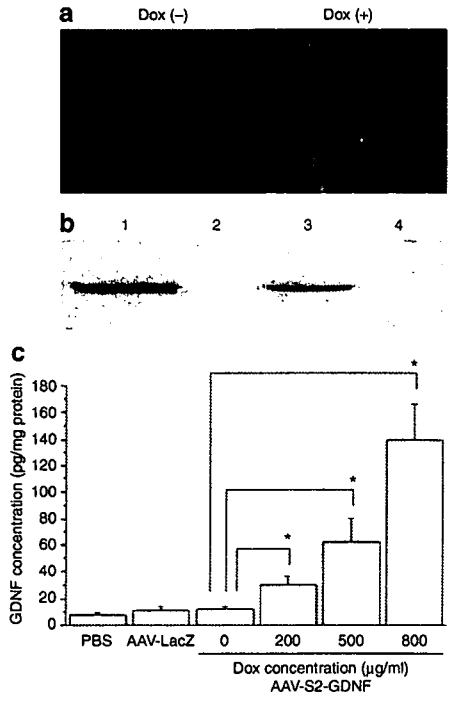

Figure 6 Induction of the transgene expression. (**a**) HEK293 cells were transfected with the proviral plasmid pAAV2-rtTA-S2-TRE-d2EGFP, and the expression of enhanced green fluorescent protein (EGFP) was induced by the doxycycline (Dox) (1 μg/ml). (**b**) Western blot analysis with an anti-FLAG antibody to detect the glial cell line–derived neurotrophic factor (GDNF) expression in the transduced 293 cells with the proviral plasmids. pAAV2-GDNF (lane 1), pAAV2-EGFP (lane 2), pAAV2-rtTA2s-S2-TRE-GDNF with Dox (lane 3), and pAAV2-rtTA2s-S2-TRE-GDNF without Dox (lane 4). (**c**) Dose–response of GDNF in the AAV2-S2-GDNF-injected muscle to the various concentrations of Dox. Mice were injected with phosphate-buffered saline (PBS), AAV2-LacZ, or AAV2-S2-GDNF followed by Dox administered in the drinking water. The mean muscle GDNF concentration in the animals treated with the AAV2-S2-GDNF in the absence of Dox was not significantly different compared to the animals treated with PBS or AAV2-*LacZ* ($P > 0.05$). The GDNF expression levels in the animals transduced with the AAV2-S2-GDNF significantly increased with increasing Dox concentration ($P < 0.05$). AAV1, adeno-associated virus 1.

In contrast, no detectable GDNF expression was observed in the cochlea of the AAV1-S2-GDNF/kanamycin group in the absence of Dox (data not shown).

Protection of cochlear function with induced GDNF expression

To evaluate the adverse effects of the transduction procedure, ABR recordings were performed on kanamycin-free rats after injection of the inducible AAV1-S2-GDNF vectors and Dox administration. At all frequencies tested, no significant increase in the ABR threshold was observed after virus injection (**Figure 8a**). This result indicates that AAV1 vector injection, transgene expression, and Dox administration did not affect the ABR threshold of the experimental rats. Interestingly, even if AAV1-S2-GDNF was injected into the cochlea of one ear, the cochleas of both ears were protected in the presence of Dox. In particular, the ABR threshold shifts were significantly improved in both the AAV1-S2-GDNF-injected cochlea of the kanamycin-treated rats in the presence of Dox (**Figure 8b**)

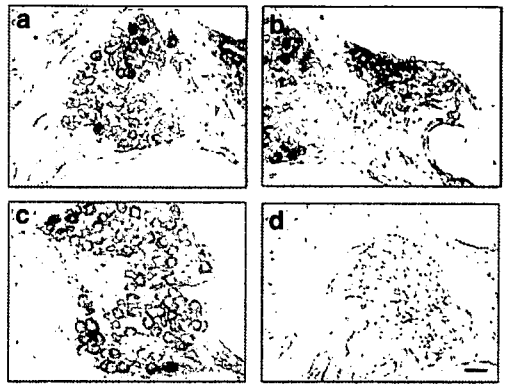

Figure 7 Expression of the GDNFflag in the rat cochlea. (**a**, **b**, **c**) The sections were sampled after the AAV1-S2-GDNF injection into the cochlea in the presence of doxycycline. GDNFflag expression was detected using an anti-FLAG antibody. (**d**) Samples from AAV1-EGFP-inoculated cochlea were analyzed as the negative control. Scale bar = 25 μm; ×400. AAV1, adeno-associated virus 1; GDNF, glial cell line–derived neurotrophic factor; EGFP, enhanced green fluorescent protein.

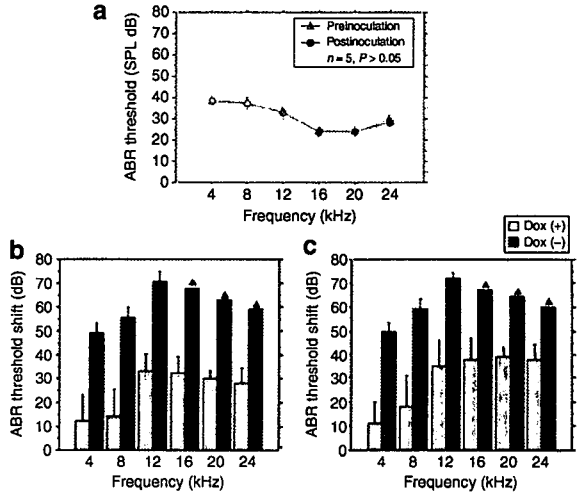

Figure 8 Protection of cochlear function with induced glial cell line–derived neurotrophic factor (GDNF) expression. (**a**) Auditory brain stem response (ABR) thresholds (mean ± SD) at each frequency tested in the AAV1-S2-GDNF-injected rat cochlea in the presence of doxycycline (Dox). No significant difference in the hearing thresholds was observed at each frequency between preinjection and postinjection. SPL, sound pressure level. ABR threshold shifts (mean ± SD) at each tested frequency in the (**b**) transduced or (**c**) nontransduced cochlea with or without Dox. Significant differences in the hearing threshold shifts were observed at each frequency between AAV1-S2-GDNF cochlea in the presence and absence of Dox ($n = 5$, $P < 0.05$). Arrows indicate the average ABR thresholds that exceeded the output power of the ABR apparatus.

and the cochlea of the noninjected contralateral ear (**Figure 8c**). However, the ABR threshold shifts at all frequencies were significantly lower in the treated group (AAV1-S2-GDNF/kanamycin plus Dox) than in the contralateral, untreated ear.

DISCUSSION

In this study, we showed that both sustained and regulated AAV1-mediated GDNF expression protected the cochlear function of rats from aminoglycoside-induced ototoxicity. Indeed, damaged spiral ganglion cells and hair cells were significantly reduced by

regulated GDNF expression. The ABR monitoring revealed that there was no loss of the cochlear function over the frequencies tested after AAV vector injection and Dox treatment. These data suggest that regulated expression of GDNF in the cochlea efficiently preserves the cochlea from kanamycin-induced ototoxicity.

Among the various viral vector systems, the recombinant AAV-mediated gene transduction system offers several important advantages as a tool for direct somatic gene delivery into the cochlea. These include long-term stable expression of therapeutic genes in a wide variety of postmitotic tissues and minimal vector-related cytotoxicity.[26] In our previous report, we demonstrated the effective transduction of mouse cochleae with the AAV1-based vectors.[7] Generally the therapeutic effectiveness depends on an appropriate concentration and the half-life of the molecules. AAV vector–mediated gene transfer is a promising delivery technique to facilitate a long-term and chronic supply of therapeutic proteins that have a short half-life, such as GDNF. Furthermore, when the CAG promoter is used, efficient transduction activity is observed in the cochlear cells including the inner hair cells and spiral ganglion cells.[27,28]

Our data showed that AAV1-GDNF-mediated transduction of the rat cochleae provided significant protection of the cochlea against aminoglycoside-induced damage. This finding is consistent with previous studies that have used adenovirus-mediated GDNF expression[13,15,16] and demonstrates the feasibility of gene therapy with AAV1-based vectors for drug-induced hearing loss. Although the exact mechanism has not yet been elucidated, antioxidant pathways might be involved in the protective function of GDNF in the inner ear.[29] Free-radical formation following exposure to aminoglycoside is considered one of the major mechanisms to explain the aminoglycoside-related hair cell death.[1,30,31] It has been previously shown that GDNF is endogenously synthesized in the inner hair cells and spiral ganglion cells of the cochlea,[32] and the two known GDNF receptors are present in the spiral ganglion.[17,32,33] In the present study, we inoculated the cochlea with the AAV1 vectors via the round window membrane and detected a high level of transgene expression mainly in the inner hair cells and spiral ganglion cells. The AAV1-mediated GDNF expression pattern was similar to that of the endogenous protein; therefore GDNF supplemented *in situ* can play a substantial role in protection. Although the transduction of the *GDNF* gene was not observed in outer hair cells, GDNF levels in the perilymph of the manipulated cochleae was much higher than in the control cochleae. These cells may respond to the secretion of another growth factor that promotes hair cell survival. Upregulation of GDNF in inner hair cells and spiral ganglion cells following noise also support this concept.[34]

Compared to the vehicle controls, increased cochlear cell survival was observed in the contralateral ears of the AAV1-GDNF group, suggesting that the contralateral cochleae in treated rats were also moderately protected. Expression of the transgene was detected in the contralateral cochlea of the rats after injection with 5×10^{10} genome copies of AAV1 per cochlea (data not shown). AAV can diffuse from one ear to the other via the cerebrospinal fluid in rodents.[35] Therefore, secreted GDNF molecules may also diffuse and exert a protective effect in the opposite ear. Alternatively, GDNF might enhance the neuronal activity (either afferent or efferent) of both ears, protecting both the treated and the contralateral cochlear function. Moreover, since infusion of the vectors into the cochlea forces large amounts of the vectors into the cerebrospinal fluid, any functional effect might be associated with the transduction of the brain. In this context, it is of great interest to know whether the otoprotective effect was achieved by the simple diffusion of the transgene product or direct transduction of the cells in the contralateral ear. To answer this question, we analyzed the local expression of the nonsecretory protein marker in the rodents with this transduction approach. Consequently, we feel that the direct transduction of the cells in the contralateral ear might be involved in the neuroprotection.

The present results showed that AAV-mediated delivery of a Tet-on system was able to control transgene expression. This Tet-on system incorporates the mutant transactivator rtTA2s-S2 and the transgene in which messenger RNA transcription is activated in the presence of an inducer, leading to protein expression. As we showed, the inducible expression of GDNF efficiently protected the cochlear structure and function from kanamycin-induced damage. GDNF was overexpressed in the induced state with the rtTA2s-S2 system, whereas GDNF expression was nearly normal in the non-induced state. In our study, cochlear function was significantly protected from aminoglycoside-induced cochlear damage in the presence of Dox. Although intracochlear injections did not affect physiological cochlear function, intramuscular injections of the vectors expressing Dox-dependent activators may elicit a cellular and humoral response against the transactivator in nonhuman primates.[36–38] The use of tissue-specific promoters that restrict transgene expression to nonprofessional antigen-presenting cells, and the use of AAV vectors, may reduce the induction of a specific T-cell response.[39]

Another attractive feature of the Tet-on system is the high safety profile of the inducer. In our study, Dox was orally administered to the rats to induce GDNF expression. Transgene expression levels were dependent on the dose of Dox, and the dose range of this inducer was below the normal bactericidal treatment levels used in similarly sized animals.[40,41] Furthermore, a Dox regimen in mice that is proportional to a clinically accepted dose of the drug in humans causes a significant induction of transgene expression.

Sequences of antibiotic administration and withdrawal to reverse the Dox induction of therapeutic gene expression were demonstrated in previous studies.[25,42] However, the aminoglycoside-induced hearing impairment model is not an appropriate model for adding and removing the Dox diet because the insulting phase is too short to successively induce and repress the Tet-on system. Furthermore, treatment of age-related hearing loss or genetic hearing loss ideally needs long-term gene expression studies to exclude any adverse events associated with the therapeutic genes.

Efficient control of the tetracycline-regulatory system is based on the specificity of the TetR/tetO interaction and the efficiency and safety of its inducers, such as tetracycline or Dox.[43,44] Mutant tTA2s are composed of one TetR and three repeated oligonucleotides of the VP-16-derived minimal activation domain. In the Tet-on system, rtTA2s-S2 showed a high activating ratio because its background expression level was lower than that of other mutants, such as rtTA2s-M2, which despite having a higher activation potential had also a high initial background.[25] By using the mutant transactivator, Urlinger *et al.* demonstrated that stringent regulation of target genes could be achieved over a range of four to five orders of magnitude

in stably transfected HeLa cells.[24] These regulatory systems could be further optimized to offer several potential advantages. The tetracycline-dependent transcriptional silencer allows tight regulation of transgene expression by eliminating baseline leakage.[20,45] Gene regulation mediated by rtTA2s-S2 was substantially tighter when combined with active silencing by the tetracycline-dependent transcriptional silencer in the non-induced state.[41,46]

Our results show that AAV1-mediated gene transfer is a promising gene delivery approach for the inner ear apparatus. To become an efficient and safe therapeutic method, it will be necessary to improve vector technology to achieve long-term transduction in a fail-safe system. We presented data demonstrating successful AAV-mediated transfer and modulation of transgene expression in the cochlea using a modified Tet-on system. In addition to the need for dosage control of neurotrophic factors, the AAV1 and the Tet-on system maybe useful for the regulation of the expression of other therapeutic gene products in the cochlea. Following further improvements, the rAAV-mediated transduction system may be of potential use for cochlear gene therapy applications in humans.

MATERIALS AND METHODS

Construction and preparation of the plasmids. The AAV vector proviral plasmid pAAV2-CAG-EGFP-WPRE (pAAV2-EGFP) contained the *EGFP* gene under the control of the CAG promoter and the WPRE and was flanked by inverted terminal repeats. A *Bam*HI fragment containing the GDNFflag complementary DNA was subcloned into this plasmid to obtain the pAAV2-CAG-GDNF-WPRE (pAAV2-GDNF) cassette.

The pAAV2-CMV-GDNFflag plasmid with the CMV promoter, the first intron of the human growth hormone gene, and the simian virus 40 polyadenylation signal sequence, were inserted between the inverted terminal repeats of the AAV type 2 genome.[47] The transactivator rtTA2s-S2 complementary DNA in the pUHrT61-1 plasmid (BD Biosciences, San Jose, CA) and the TRE in the pTRE-d2EGFP plasmid (BD Biosciences, CA) were subcloned together into the pAAV2-CMV-GDNFflag plasmid to obtain the AAV vector proviral plasmid pAAV2-rtTA2s-S2-TRE-GDNF. A *Sac*II-*Eco*RI fragment containing the d2EGFP complementary DNA from the pTRE-d2EGFP plasmid (BD Biosciences, CA) was subcloned into this plasmid to create the pAAV2-rtTA2s-S2-TRE-EGFP plasmid (see **Supplementary Materials and Methods**).

Recombinant AAV vector production. The AAV1 vectors were produced as previously described by using a 293-cell transfection protocol[26] with the proviral plasmid pAAV2-EGFP, pAAV2-Luciferase,[48] pAAV2-GDNF, pAAV2-rtTA2s-S2-TRE-EGFP, or pAAV2-rtTA2s-S2-TRE-GDNF; the AAV packaging plasmid pAAV1RepCap; and the adenovirus helper plasmid pAdeno5 using an active gassing system.[49] The recombinant AAV2 expressing the *Escherichia coli* β-galactosidase gene under the control of the CMV promoter (AAV2-LacZ) was generated using the proviral plasmid pAAV-LacZ.[50] (see **Supplementary Materials and Methods**).

In vitro *expression of GDNF.* To detect the *in vitro* expression of the GDNFflag fusion protein, 293 cells were transduced with the AAV1-GDNFflag at 1×10^4 vector genome copies/cell. For the detection of the regulated expression, 293 cells were transduced with the AAV proviral plasmid pAAV2-rtTA2s-S2-TRE-d2EGFP or pAAV2-rtTA2s-S2-TRE-GDNF in the presence or absence of 1 μmol/l Dox-HCl (Sigma, St Louis, MO) (see **Supplementary Materials and Methods**).

Surgical procedures and cochlear perfusions. All animal studies were performed in accordance with the guidelines issued by the committee on animal research at Jichi Medical University. Twenty 5-week-old male Sprague–Dawley rats with normal Preyer's reflexes weighing 130–150g were utilized (CLEA Japan, Tokyo, Japan). Five-week-old male C57BL/6J mice were utilized for optical bioluminescence imaging. The animals were anesthetized with ketamine (50 mg/kg) and xylazine (5 mg/kg). A postauricular approach was performed to expose the tympanic bony bulla. A small opening (2 mm in diameter) to the tympanic bulla was made by carefully drilling through the bone of the bulla to gain access to the round window membrane. Subsequently, 5 μl of AAV vector solution (AAV1-EGFP, AAV2-Luciferase, or AAV1-GDNF, 5×10^{10} genome copies, $n = 5$ each) was microinjected into the cochlea through the round window for over 10 minutes using a glass micropipette (40 μm in diameter) fitted on a Univentor 801 syringe pump (Serial No. 170182, High Precision Instruments, Univentor Ltd., Malta). The rats were also injected with the AAV1-S2-GDNF in the presence ($n = 5$) or absence ($n = 5$) of Dox. A small plug of muscle was used to seal the cochlea, and the surgical wound was closed in layers and dressed with an antibiotic ointment.

***Transgene expression* in vivo.** The rats were deeply anesthetized and the perilymph was sampled from the inoculated cochlea through the round window. GDNF protein levels were measured using a GDNF Emax ImmunoAssay System (Promega, Madison, WI) according to the manufacturer's instructions. The GDNF expression in the rat cochlea was determined by immunohistochemistry using an anti-FLAG antibody.

AAV2-LacZ or AAV2-S2-GDNF vector (1×10^{10} genome copies) was injected into the quadriceps of the C57BL/6J mice (6 weeks old, CLEA Japan, Tokyo, Japan). The mice were injected with phosphate-buffered saline ($n = 5$) or AAV2-*LacZ* ($n = 5$). Animals treated with various concentrations of Dox were injected with the AAV2-S2-GDNF ($n = 5$ per group). Two weeks after the transduction, animals were deeply anesthetized, and the injected muscle was sampled. The tissue levels of the GDNF protein were measured with an enzyme-linked immunosorbent assay kit (GDNF Emax ImmunoAssay System, Promega, WI), according to the manufacturer's instructions. The levels of GDNF were expressed as pg/mg protein. The assay sensitivity ranged from 16 to 1,000 pg/ml.

Two weeks after the injection of the AAV2-Luciferase, optical bioluminescence imaging was performed using the CCD camera (Xenogen, Alameda, CA). After intraperitoneal injection of reporter substrate D-Luciferin (375 mg/kg body weight), mice were imaged for scans.

Kanamycin administration and ABR assessment. A dose of 333 mg of kanamycin base/kg body weight was obtained by injecting 3 μl/g body weight. Seven days after virus injection, kanamycin was given subcutaneously twice daily for 12 consecutive days. The body weight of the animals was monitored daily to adjust the kanamycin dosages accordingly.

Auditory thresholds were determined by audiometry of evoked ABRs using Tucker-DAVIS Technologies and Scope software (Power Lab; ADInstruments, Coloado Springs, CO). Thresholds were evaluated for each animal prior to the start of the injection procedure and 2 days after the termination of kanamycin treatment. The ABRs were measured as previously described,[7] using a two-way repeated analysis of variance (see **Supplementary Materials and Methods**).

Histological evaluation of the cochlear preservation. Cochlear hair cell loss was determined by F-actin staining. One month after transduction, the presence of the cochlear spiral ganglion neurons was determined by 4′,6-diamino-2-phenylindole dihydrochloride staining to visualize nuclear chromatin. After decalcification, 6 μm mid-modiolus cryosections of the cochleae from each animal were histologically analyzed. The number of spiral ganglion neurons was determined in every third section of the cochlear basal turn from the AAV1-transduced and kanamycin-treated rats (see **Supplementary Materials and Methods**).

Statistical analyses. Results are presented as the means ± SD. Data were statistically analyzed using analysis of variance, paired student's *t*-test (injected versus contralateral sides) or unpaired student's *t*-test (therapy versus control groups) (StatView 5.0 software; SAS Institute, Cary, NC).

ACKNOWLEDGMENTS

The authors thank Avigen. (Alameda, CA) for providing the pAAV-LacZ and pAdeno. We also thank Thomas Hope (Department of Microbiology and Immunology, The University of Illinois at Chicago) for providing pBS II SK+WPRE-B11 and Jun-Ichi Miyazaki (Osaka University Graduate School of Medicine, Osaka, Japan) for pCAGGS. The authors also thank Miyoko Mitsu for her encouragement and technical support. This work was supported in part by grants from the Ministry of Health, Labour and Welfare of Japan (Grants-in-Aid for Scientific Research and grant for 21 Century Centers of Excellence program) and the "High-Tech Research Center" Project for Private Universities (matching fund subsidy, from the Ministry of Education, Culture, Sports, Science, and Technology of Japan). The authors declare no conflict of interest.

SUPPLEMENTARY MATERIAL

Materials and Methods.

Figure S1. Bioluminescence of the transduced cochlea in living mice.

REFERENCES

1. Wu, WJ, Sha, SH and Schacht, J (2002). Recent advances in understanding aminoglycoside ototoxicity and its prevention. *Audiol Neurootol* **7**: 171–174.
2. Hellier, WP, Wagstaff, SA, O'Leary, SJ and Shepherd, RK (2002). Functional and morphological response of the stria vascularis following a sensorineural hearing loss. *Hear Res* **172**: 127–136.
3. Tsue, TT, Oesterle, EC and Rubel, EW (1994). Hair cell regeneration in the inner ear. *Otolaryngol Head Neck Surg* **111**: 281–301.
4. Raphael, Y, Frisancho, JC and Roessler, BJ (1996). Adenoviral-mediated gene transfer into guinea pig cochlear cells *in vivo*. *Neurosci Lett* **207**: 137–141.
5. Ishimoto, S, Kawamoto, K, Kanzaki, S and Raphael, Y (2002). Gene transfer into supporting cells of the organ of Corti. *Hear Res* **173**: 187–197.
6. Okada, T, Nomoto, T, Shimazaki, K, Lijun, W, Lu, Y, Matsushita, T *et al.* (2002). Adeno-associated virus vectors for gene transfer to the brain. *Methods* **28**: 237–247.
7. Liu, Y, Okada, T, Sheykholeslami, K, Shimazaki, K, Nomoto, T, Muramatsu, SI *et al.* (2005). Specific and efficient transduction of cochlear inner hair cells with recombinant adeno-associated virus type 3 vector. *Mol Ther* **12**: 725–733.
8. Lin, LF, Doherty, DH, Lile, JD, Bektesh, S and Collins, F (1993). GDNF: a glial cell line-derived neurotrophic factor for midbrain dopaminergic neurons. *Science* **260**: 1130–1132.
9. Henderson, CE, Phillips, HS, Pollock, RA, Davies, AM, Lemeulle, C, Armanini, M *et al.* (1994). GDNF: a potent survival factor for motoneurons present in peripheral nerve and muscle. *Science* **266**: 1062–1064.
10. Wang, Y, Lin, SZ, Chiou, AL, Williams, LR and Hoffer, BJ (1997). Glial cell line-derived neurotrophic factor protects against ischemia-induced injury in the cerebral cortex. *J Neurosci* **17**: 4341–4348.
11. Keithley, EM, Ma, CL, Ryan, AF, Louis, JC and Magal, E (1998). GDNF protects the cochlea against noise damage. *Neuroreport* **9**: 2183–2187.
12. Shoji, F, Yamasoba, T, Magal, E, Dolan, DF, Altschuler, RA and Miller, JM (2000). Glial cell line-derived neurotrophic factor has a dose dependent influence on noise-induced hearing loss in the guinea pig cochlea. *Hear Res* **142**: 41–55.
13. Suzuki, M, Yagi, M, Brown, JN, Miller, AL, Miller, JM and Raphael, Y (2000). Effect of transgenic GDNF expression on gentamicin-induced cochlear and vestibular toxicity. *Gene Ther* **7**: 1046–1054.
14. Yagi, M, Kanzaki, S, Kawamoto, K, Shin, B, Shah, PP, Magal, E *et al.* (2000). Spiral ganglion neurons are protected from degeneration by GDNF gene therapy. *J Assoc Res Otolaryngol* **1**: 315–325.
15. Hakuba, N, Watabe, K, Hyodo, J, Ohashi, T, Eto, Y, Taniguchi, M *et al.* (2003). Adenovirus-mediated overexpression of a gene prevents hearing loss and progressive inner hair cell loss after transient cochlear ischemia in gerbils. *Gene Ther* **10**: 426–433.
16. Kawamoto, K, Yagi, M, Stover, T, Kanzaki, S and Raphael, Y (2003). Hearing and hair cells are protected by adenoviral gene therapy with TGF-beta1 and GDNF. *Mol Ther* **7**: 484–492.
17. Kuang, R, Hever, G, Zajic, G, Yan, Q, Collins, F, Louis, JC *et al.* (1999). Glial cell line-derived neurotrophic factor. Potential for otoprotection. *Ann NY Acad Sci* **884**: 270–291.
18. Yagi, M, Magal, E, Sheng, Z, Ang, KA and Raphael, Y (1999). Hair cell protection from aminoglycoside ototoxicity by adenovirus-mediated overexpression of glial cell line-derived neurotrophic factor. *Hum Gene Ther* **10**: 813–823.
19. Meng, X, Lindahl, M, Hyvonen, ME, Parvinen, M, de Rooij, DG, Hess, MW *et al.* (2000). Regulation of cell fate decision of undifferentiated spermatogonia by GDNF. *Science* **287**: 1489–1493.
20. Perez, N, Plence, P, Millet, V, Greuet, D, Minot, C, Noel, D *et al.* (2002). Tetracycline transcriptional silencer tightly controls transgene expression after *in vivo* intramuscular electrotransfer: application to interleukin 10 therapy in experimental arthritis. *Hum Gene Ther* **13**: 2161–2172.
21. Regulier, E, Pereira de Almeida, L, Sommer, B, Aebischer, P and Deglon, N (2002). Dose-dependent neuroprotective effect of ciliary neurotrophic factor delivered via tetracycline-regulated lentiviral vectors in the quinolinic acid rat model of Huntington's disease. *Hum Gene Ther* **13**: 1981–1990.
22. Rubinchik, S, Worarataanadharm, J, Yu, H and Dong, JY (2005). New complex Ad vectors incorporating both rtTA and tTS deliver tightly regulated transgene expression both *in vitro* and *in vivo*. *Gene Ther* **12**: 504–511.
23. Pluta, K, Luce, MJ, Bao, L, Agha-Mohammadi, S and Reiser, J (2005). Tight control of transgene expression by lentivirus vectors containing second-generation tetracycline-responsive promoters. *J Gene Med* **7**: 803–817.
24. Urlinger, S, Baron, U, Thellmann, M, Hasan, MT, Bujard, H and Hillen, W (2000). Exploring the sequence space for tetracycline-dependent transcriptional activators: novel mutations yield expanded range and sensitivity. *Proc Natl Acad Sci USA* **97**: 7963–7968.
25. Lamartina, S, Roscilli, G, Rinaudo, CD, Sporeno, E, Silvi, L, Hillen, W *et al.* (2002). Stringent control of gene expression *in vivo* by using novel doxycycline-dependent trans-activators. *Hum Gene Ther* **13**: 199–210.
26. Okada, T, Shimazaki, K, Nomoto, T, Matsushita, T, Mizukami, H, Urabe, M *et al.* (2002). Adeno-associated viral vector-mediated gene therapy of ischemia-induced neuronal death. *Methods Enzymol* **346**: 378–393.
27. Stone, IM, Lurie, DI, Kelley, MW and Poulsen, DJ (2005). Adeno-associated virus-mediated gene transfer to hair cells and support cells of the murine cochlea. *Mol Ther* **11**: 843–848.
28. Liu, Y, Okada, T, Nomoto, T, Ke, X, Kume, A, Ozawa, K *et al.* (2007). Promoter effects of adeno-associated viral vector for transgene expression in the cochlea *in vivo*. *Exp Mol Med* **39**: 170–175.
29. Oppenheim, RW (1997). Related mechanisms of action of growth factors and antioxidants in apoptosis: an overview. *Adv Neurol* **72**: 69–78.
30. Priuska, EM and Schacht, J (1995). Formation of free radicals by gentamicin and iron and evidence for an iron/gentamicin complex. *Biochem Pharmacol* **50**: 1749–1752.
31. Sha, SH and Schacht, J (1999). Stimulation of free radical formation by aminoglycoside antibiotics. *Hear Res* **128**: 112–118.
32. Sanicola, M, Hession, C, Worley, D, Carmillo, P, Ehrenfels, C, Walus, L *et al.* (1997). Glial cell line-derived neurotrophic factor-dependent RET activation can be mediated by two different cell-surface accessory proteins. *Proc Natl Acad Sci USA* **94**: 6238–6243.
33. Ylikoski, J, Pirvola, U, Virkkala, J, Suvanto, P, Liang, XQ, Magal, E *et al.* (1998). Guinea pig auditory neurons are protected by glial cell line-derived growth factor from degeneration after noise trauma. *Hear Res* **124**: 17–26.
34. Nam, YJ, Stover, T, Hartman, SS and Altschuler, RA (2000). Upregulation of glial cell line-derived neurotrophic factor (GDNF) in the rat cochlea following noise. *Hear Res* **146**: 1–6.
35. Kho, ST, Pettis, RM, Mhatre, AN and Lalwani, AK (2000). Safety of adeno-associated virus as cochlear gene transfer vector: analysis of distant spread beyond injected cochleae. *Mol Ther* **2**: 368–373.
36. Favre, D, Blouin, V, Provost, N, Spisek, R, Porrot, F, Bohl, D *et al.* (2002). Lack of an immune response against the tetracycline-dependent transactivator correlates with long-term doxycycline-regulated transgene expression in non-human primates after intramuscular injection of recombinant adeno-associated virus. *J Virol* **76**: 11605–11611.
37. Latta-Mahieu, M, Rolland, M, Caillet, C, Wang, M, Kennel, P, Mahfouz, I *et al.* (2002). Gene transfer of a chimeric trans-activator is immunogenic and results in short-lived transgene expression. *Hum Gene Ther* **13**: 1611–1620.
38. Lena, AM, Giannetti, P, Sporeno, E, Ciliberto, G and Savino, R (2005). Immune responses against tetracycline-dependent transactivators affect long-term expression of mouse erythropoietin delivered by a helper-dependent adenoviral vector. *J Gene Med* **7**: 1086–1096.
39. Cordier, L, Gao, GP, Hack, AA, McNally, EM, Wilson, JM, Chirmule, N *et al.* (2001). Muscle-specific promoters may be necessary for adeno-associated virus-mediated gene transfer in the treatment of muscular dystrophies. *Hum Gene Ther* **12**: 205–215.
40. McGee Sanftner, LH, Rendahl, KG, Quiroz, D, Coyne, M, Ladner, M, Manning, WC *et al.* (2001). Recombinant AAV-mediated delivery of a tet-inducible reporter gene to the rat retina. *Mol Ther* **3**: 688–696.
41. Lamartina, S, Silvi, L, Roscilli, G, Casimiro, D, Simon, AJ, Davies, ME *et al.* (2003). Construction of an rtTA2(s)-m2/tts(kid)-based transcription regulatory switch that displays no basal activity, good inducibility, and high responsiveness to doxycycline in mice and non-human primates. *Mol Ther* **7**: 271–280.
42. Srour, MA, Fechner, H, Wang, X, Siemetzki, U, Albert, T, Oldenburg, J *et al.* (2003). Regulation of human factor IX expression using doxycycline-inducible gene expression system. *Thromb Haemost* **90**: 398–405.
43. Kistner, A, Gossen, M, Zimmermann, F, Jerecic, J, Ullmer, C, Lubbert, H *et al.* (1996). Doxycycline-mediated quantitative and tissue-specific control of gene expression in transgenic mice. *Proc Natl Acad Sci USA* **93**: 10933–10938.
44. Knott, A, Garke, K, Urlinger, S, Guthmann, J, Muller, Y, Thellmann, M *et al.* (2002). Tetracycline-dependent gene regulation: combinations of transregulators yield a variety of expression windows. *Biotechniques* **32**: 796, 798, 800 passim.
45. Rendahl, KG, Quiroz, D, Ladner, M, Coyne, M, Seltzer, J, Manning, WC *et al.* (2002). Tightly regulated long-term erythropoietin expression in vivo using tet-inducible recombinant adeno-associated viral vectors. *Hum Gene Ther* **13**: 335–342.
46. Salucci, V, Scarito, A, Aurisicchio, L, Lamartina, S, Nicolaus, G, Giampaoli, S *et al.* (2002). Tight control of gene expression by a helper-dependent adenovirus vector carrying the rtTA2(s)-M2 tetracycline transactivator and repressor system. *Gene Ther* **9**: 1415–1421.
47. Wang, L, Muramatsu, S, Lu, Y, Ikeguchi, K, Fujimoto, K, Okada, T *et al.* (2002). Delayed delivery of AAV-GDNF prevents nigral neurodegeneration and promotes functional recovery in a rat model of Parkinson's disease. *Gene Ther* **9**: 381–389.
48. Okada, T, Uchibori, R, Iwata-Okada, M, Takahashi, M, Nomoto, T, Nonaka-Sarukawa, M *et al.* (2006). A histone deacetylase inhibitor enhances recombinant adeno-associated virus-mediated gene expression in tumor cells. *Mol Ther* **13**: 738–746.
49. Okada, T, Nomoto, T, Yoshioka, T, Nonaka-Sarukawa, M, Ito, T, Ogura, T *et al.* (2005). Large-scale production of recombinant viruses by use of a large culture vessel with active gassing. *Hum Gene Ther* **16**: 1212–1218.
50. Okada, T, Mizukami, H, Urabe, M, Nomoto, T, Matsushita, T, Hanazono, Y *et al.* (2001). Development and characterization of an antisense-mediated prepackaging cell line for adeno-associated virus vector production. *Biochem Biophys Res Commun* **288**: 62–68.

Interleukin-10 Expression Mediated by an Adeno-Associated Virus Vector Prevents Monocrotaline-Induced Pulmonary Arterial Hypertension in Rats

Takayuki Ito, Takashi Okada, Hiroshi Miyashita, Tatsuya Nomoto, Mutsuko Nonaka-Sarukawa, Ryosuke Uchibori, Yoshikazu Maeda, Masashi Urabe, Hiroaki Mizukami, Akihiro Kume, Masafumi Takahashi, Uichi Ikeda, Kazuyuki Shimada, Keiya Ozawa

Abstract—Pulmonary arterial hypertension (PAH) is a fatal disease associated with inflammation and pathological remodeling of the pulmonary artery (PA). Interleukin (IL)-10 is a pleiotropic antiinflammatory cytokine with vasculoprotective properties. Here, we report the preventive effects of IL-10 on monocrotaline-induced PAH. Three-week-old Wistar rats were intramuscularly injected with an adeno-associated virus serotype 1 vector expressing IL-10, followed by monocrotaline injection at 7 weeks old. IL-10 transduction significantly improved survival rates of the PAH rats 8 weeks after monocrotaline administration compared with control gene transduction (75% versus 0%, $P<0.01$). IL-10 also significantly reduced mean PA pressure (22.8 ± 1.5 versus 29.7 ± 2.8 mm Hg, $P<0.05$), a weight ratio of right ventricle to left ventricle plus septum (0.35 ± 0.04 versus 0.42 ± 0.05, $P<0.05$), and percent medial thickness of the PA ($12.9\pm0.3\%$ versus $21.4\pm0.4\%$, $P<0.01$) compared with controls. IL-10 significantly reduced macrophage infiltration and vascular cell proliferation in the remodeled PA in vivo. It also significantly decreased the lung levels of transforming growth factor-β_1 and IL-6, which are indicative of PA remodeling. In addition, IL-10 increased the lung level of heme oxygenase-1, which strongly prevents PA remodeling. In vitro analysis revealed that IL-10 significantly inhibited excessive proliferation of cultured human PA smooth muscle cells treated with transforming growth factor-β_1 or the heme oxygenase inhibitor tin protoporphyrin IX. Thus, IL-10 prevented the development of monocrotaline-induced PAH, and these results provide new insights into the molecular mechanisms of human PAH. (*Circ Res.* **2007;101:734-741.**)

Key Words: pulmonary hypertension ■ interleukins ■ gene therapy ■ inflammation ■ vascular smooth muscle cell proliferation

Pulmonary arterial hypertension (PAH) is an intractable disease that leads to increased pulmonary arterial pressure, progressive right heart failure, and premature death; however, no satisfactory treatment for PAH has been established.[1] The pathological process of PAH is characterized by abnormal remodeling of the pulmonary artery (PA) associated with excessive proliferation of pulmonary arterial smooth muscle cells (PASMCs).[2] Accumulating evidence suggests important roles of vascular inflammation in its pathogenesis.[2,3] For instance, serum levels of proinflammatory cytokines such as interleukin (IL)-1 and IL-6 reflect the disease activity in patients with idiopathic PAH.[4] Furthermore, injection of IL-6 can produce PAH and PA remodeling in rats.[5] The remodeled PA presents macrophage infiltration and increased expression of a variety of cytokines, including IL-6, tumor necrosis factor (TNF)-α, and transforming growth factor (TGF)-β_1.[6,7] Administration of steroids or immunosuppressive drugs decreases the level of PA pressure in patients with PAH.[8,9] These observations suggest a therapeutic potential of targeting inflammation to prevent PAH progression.[10] However, the precise mechanisms underlying the antiinflammatory effects on PA remodeling have not yet been fully investigated.

IL-10 is a multifunctional antiinflammatory cytokine with a vasculoprotective property. During the course of inflammation, IL-10 is produced by type-2 helper T (Th2) lymphocytes, and it inhibits the production of various proinflammatory cytokines in macrophages and Th1 lymphocytes.[11] Exogenous IL-10 prevents proliferative vasculopathy in vivo by inhibiting inflammatory cell infiltration,[12] smooth muscle cell proliferation,[12,13] and chemokine expression.[14] However, clinical efficacy of systemic recombinant IL-10 administra-

Original received March 28, 2007; revision received July 12, 2007; accepted July 23, 2007.

From the Division of Genetic Therapeutics (T.I., T.N., M.N.-S., M.U., H.M., A.K., K.O., R.U.), the Division of Cardiovascular Medicine (T.I., H.M., M.N.-S., K.S., Y.M.), Jichi Medical University, Japan; the Department of Molecular Therapy (T.O.), National Institute of Neuroscience, National Center of Neurology and Psychiatry, Japan; and the Department of Organ Regeneration (M.T., U.I.), Shinshu University Graduate School of Medicine, Japan.

Correspondence to Takayuki Ito, MD, PhD, Division of Genetic Therapeutics, Jichi Medical University, 3311-1 Yakushiji, Shimotsuke, Tochigi 329-0498, Japan. E-mail titou@jichi.ac.jp

Circulation Research is available at http://circres.ahajournals.org

DOI: 10.1161/CIRCRESAHA.107.153023

tion are insufficient because of the lower local IL-10 levels resulting from its short bioactive half-life.[15] In this study, we used an adeno-associated virus (AAV) vector for IL-10 expression because it is an efficient vehicle for systemic and sustained expression of therapeutic proteins.[14] It also has an advantage over other viral vectors in the therapeutic or mechanistic analysis because it produces minimal inflammatory and immune responses in vivo.

Recently, heme oxygenase (HO)-1, an inducible form of HO that promotes production of a vasodilator carbon monoxide (CO), was shown to mediate antiinflammatory and antiproliferative effects of IL-10 in a model of chronic vasculopathy.[12] Increased HO-1 and CO levels attenuated PAH and PA remodeling by inhibiting PASMC proliferation.[16–18] However, no study has explored a direct link between IL-10 and HO-1 in the pathogenesis of PAH. Thus, we examined the effects of IL-10, delivered via an AAV vector, on PA remodeling in a widely-used rat model of PAH induced by the pyrolizidine alkaloid monocrotaline (MCT). We also investigated the mechanisms underlying the effects of IL-10 on the following factors involved in the inflammatory and proliferative vascular changes in PAH: PASMC, macrophage, TGF-β_1, IL-6, and HO-1.

Materials and Methods

AAV Vector Production

DNA encoding rat IL-10 was polymerase chain reaction-amplified from rat splenocyte complementary DNA, using the primers 5′-GCACGAGAGCCACAACGCA-3′ and 5′-GATTTGAGTACG-ATCCATTTATTCAAAACGAGGAT-3′. For efficient transgene expression in the skeletal muscle, we constructed a recombinant AAV vector which carried the IL-10 gene (AAV-IL-10) or enhanced green fluorescent protein (eGFP) gene (AAV-eGFP), controlled by the modified chicken β-actin promoter with the cytomegalo virus-immediate early enhancer and the woodchuck hepatitis virus post-transcriptional regulatory element (a kind gift from Dr Thomas Hope, Infectious Disease Laboratory, Salk Institute). AAV vectors were prepared according to the previously described 3-plasmid transfection adenovirus-free protocol with minor modifications to use the active gassing system.[19,20] In brief, 60% confluent human embryonic kidney 293 cells incubated in a large culture vessel with active air circulation were cotransfected with the proviral transgene plasmid, AAV-1 chimeric helper plasmid (p1RepCap), and adenoviral helper plasmid pAdeno (Avigen Inc). The crude viral lysate was purified by 2 rounds of cesium chloride 2-tier centrifugation.[21] The viral stock titer was determined against plasmid standards by dot blot hybridization, after which the stock was dissolved in HN buffer (50 mmol/L HEPES, pH 7.4, 0.15 mol/L NaCl) before injection.

Animal Models

All animal experiments were approved by the Jichi Medical University ethics committee and were performed in accordance with the *National Institute of Health Guide for the Care and Use of Laboratory Animals*. To evaluate the efficiency of in vivo gene expression, 3-week-old male Wistar rats (Clea Japan Inc, Tokyo, Japan) weighing 45 to 55 g were injected with AAV-IL-10 (200 μL, 3×10^{10} to 1×10^{11} genome copies [g.c.] per body) into the bilateral anterior tibial muscles (n=3 animals per group). For hemodynamic and histological analysis, we randomly formed 4 groups comprising 5 rats each: sham rats that were administered the HN buffer (1, NC group); MCT-treated rats administered the HN buffer (2, MCT group); MCT rats administered AAV-eGFP (3, MCT+eGFP group); and MCT rats administered AAV-IL-10 (4, MCT+IL-10 group). After anesthetized with a spontaneous inhalation of 1% isoflurane, the rats in the groups 3 and 4 received intramuscular injection of AAV-eGFP or AAV-IL-10 (200 μL, 6×10^{10} g.c. per body), respectively. Rats in groups 1 and 2 were injected with the HN buffer (200 μL). MCT (Wako Pure Chemicals) was dissolved in 0.1N HCl, and the pH adjusted to 7.4 with 1.0N NaOH. For hemodynamic and histological studies, all rats except those in the NC group were subcutaneously injected with MCT (30 mg/kg) under the spontaneous inhalation of 1% isoflurane at 4 weeks after vector treatment. For the survival study, rats (n=8 animals/group) were injected with a lethal dose of MCT (45 mg/kg) under the spontaneous inhalation of 1% isoflurane at 4 weeks after vector injection. Survival was estimated from the date of MCT injection until death or 8 weeks after injection.

Hemodynamic Analysis

Four weeks after MCT injection, the rats were anesthetized with spontaneous inhalation of 1% isoflurane, and a tracheotomy was performed. Then, they were mechanically ventilated using a respirator (SAR-830/AP, CWE; tidal volume: 10 mL/kg, respiratory rate: 30 breaths per min) and anesthetized with 0.5% isoflurane through a tracheostomy. After the thoracic cavity was opened using a midsternal approach, 2.0F high-fidelity manometer-tipped catheters (SPC-320, Millar Instruments Inc) were inserted directly into the right or left ventricle. The mean pulmonary arterial pressure (mPAP) or mean aortic arterial pressure (mAoP) was measured using the catheters that were advanced from the right or left ventricle, respectively. The heart rate (HR) was measured by unipolar lead electrocardiography.

Ventricular Weight Measurement and Morphometric Analysis of the PA

After hemodynamic analysis, the rats were euthanized using an overdose isoflurane (5%). The lungs and PAs were perfused with 5 mL of saline followed by 10 mL of cold 4% paraformaldehyde. Each ventricle and the lungs were excised, dissected free, and weighed. The weight ratio of right ventricle to the left ventricle plus septum [RV/(LV+S)] was calculated as an index of right ventricular hypertrophy (RVH). The tissues were fixed in 4% paraformaldehyde for 4 hours, transferred to 30% sucrose in 0.1 mol/L phosphate buffer (pH 7.4) for cryoprotection, and stored at 4°C overnight. Lung tissue was frozen in Tissue-Tek OCT compound (Sakura Finetechnical Co) at −20°C. Then, 7-μm sections were cut using a cryostat. Hematoxylin and eosin (HE) staining was performed on sections from the middle lobe of the right lung, and these were examined using light microscopy. Morphometric analysis was performed in PAs with an external diameter of 25 to 50 and 51 to 100 μm. The medial wall thickness was calculated with the following formula: medial thickness (%)=medial wall thickness/external diameter×100.[22] For quantitative analysis, 30 vessels from each rat were counted and the average was calculated.

Immunohistochemistry

Immunohistochemical staining was performed with monoclonal antibodies against ED1 (1:100; Serotec) and proliferating cell nuclear antigen (PCNA, 1:200; Zymed), using the streptavidin-biotin-peroxidase method, as described previously.[23] ED1 recognizes the lysosomal membrane antigen expressed by a majority of tissue macrophages. Irrelevant mouse immunoglobulin G (Vector Laboratories) was used as a negative control. Reactions were visualized using Vector SG (Vector Laboratories) or 3,3′-diaminobenzidine (Zymed) and counterstained with nuclear fast red or hematoxylin. The number of ED1-positive cells was counted in 250×250-μm fields under 400× magnification and expressed as cells per mm^2. The number of PCNA-positive cells was quantitatively evaluated as a percentage of total vascular cells in the fields under 1000× magnification. For each rat, the average number or percentage of each cell in 15 randomly selected fields was used for statistical analysis.

Protein Assay

Protein samples were prepared by homogenization of the frozen lung tissue in lysis buffer [10 μmol/L Tris/Cl (pH 8.0), 0.2% NP-40,